VALIDATION OF THE *PYRENOPHORA TERES* F. *TERES PTTBEE1* REGION AND MAPPING OF RESISTANCE TO *P. TERES* F. *MACULATA* IN DURUM

A Thesis
Submitted to the Graduate Faculty
of the
North Dakota State University
of Agriculture and Applied Science

By

Ryan Michael Skiba

In Partial Fulfillment of the Requirements
for the Degree of
MASTER OF SCIENCE

Major Program:
Genomics and Bioinformatics

November 2021

Fargo, North Dakota

North Dakota State University

Graduate School

Title

VALIDATION OF THE *PYRENOPHORA TERES* F. *TERES PTTBEE1* REGION AND MAPPING OF RESISTANCE TO *P. TERES* F. *MACULATA* IN DURUM

By

Ryan Skiba

The Supervisory Committee certifies that this ***disquisition*** complies with North Dakota State University's regulations and meets the accepted standards for the degree of

MASTER OF SCIENCE

SUPERVISORY COMMITTEE:

Dr. Phillip E. McClean

Chair

Dr. Timothy Friesen

Dr. Zhaohui Liu

Approved:

11/11/2021

Date

Dr. Phillip E. McClean

Department Chair

ABSTRACT

Pyrenophora teres is a fungal pathogen of barley and other closely related grass species. Two forms of the pathogen, *P. teres* f. *teres* and *P. teres* f. *maculata*, are the causative agents of net form net blotch and spot form net blotch of barley, respectively. Genetic and bioinformatic approaches were used to identify eight candidate effectors in the *P. teres* f. *teres PttBee1* region. Genes were validated using CRISPR-Cas9 mediated gene disruptions. As no transformants displayed alterations in virulence, additional markers were implemented into a *P. teres* f. *teres* genetic map to refine the locus. As *P. teres* f. *maculata* has recently emerged as a pathogen of wheat, a quantitative trait loci analysis and genome wide association study were performed with this pathogen using a durum wheat biparental mapping population and a subset of the Global Durum Wheat Panel, respectively, both showing an association with resistance/susceptibility on chromosome 2A.

ACKNOWLEDGEMENTS

First and foremost, I would like to thank my advisor Dr. Tim Friesen for his continued support and mentorship, for teaching me how to think critically about my research, and for nurturing my growth as a scientist. I would also like to thank my current and past lab-mates, including Danielle Holmes, Dr. Nathan Wyatt, Dr. Gayan Kariyawasam, Dr. Jinling Li, Megan Engel, Emma Navratil, Ashley Nelson, and Sam Malone for putting up with my questions, helping with my experiments, and for contributing to an all-around excellent work environment. Finally, I would like to thank Dr. Phillip McClean and Dr. Zhaohui Liu for helping to guide my research, as well as the North Dakota Barley Council and USDA Northern Crop Science Laboratory for making this work possible.

DEDICATION

This thesis is dedicated to my parents Neil and Carol, for supporting me unconditionally throughout my academic career and always encouraging me to achieve my goals.

TABLE OF CONTENTS

LIST OF TABLES

LIST OF FIGURES

CHAPTER 1. LITERATURE REVIEW

1.1. Net blotch disease

First described by Atanasoff and Johnson (1920), net form net blotch (NFNB) of barley (*Hordeum vulgare*) is caused by *Pyrenophora teres* f. *teres* and is characterized by dark brown pin-point foliar lesions that progress to transverse and longitudinal necrotic streaks forming a reticulated pattern, often with accompanying chlorosis. Similarly, spot form net blotch (SFNB) caused by *Pyrenophora teres* f. *maculata* results in brown necrotic lesions within chlorotic regions, though these progress towards round or oval shaped lesions over time (Shipton et al. 1973; Smedegård-Petersen 1971). The severity of disease caused by *P. teres* is dependent on the genetics of both pathogen and host as well as environmental variables such as temperature and humidity (Liu et al. 2011). A resistant or incompatible interaction is characterized by pinpoint necrotic lesions generally unaccompanied by chlorosis, indicative of a failure of the pathogen to advance within the plant. In a highly susceptible or compatible interaction, necrotic lesions spread through the leaf to the point of coalescence. Alternatively, disease phenotypes may appear to fall between both extremes, indicating an intermediate reaction type between complete compatibility and incompatibility (Tekauz 1985).

Both forms of the pathogen are present worldwide, though one form is frequently dominant in a specific region, with the predominant form often changing over time (Liu et al. 2010; Louw et al. 1996; McLean et al. 2009). The virulence profile of a *P. teres* population is liable to change in response to the introduction of a resistant host background (Khan 1982). Though most of the research into net blotch has historically focused on *P. teres* f. *teres,* the recent prominence of SFNB in US (Liu et al. 2010; Marshall et al. 2015) and Australian (McClean et al. 2010) barley growing regions, as well as the emergence of susceptibility in

wheat (*Triticum* L.) (Mikhailova et al. 2010; Perelló et al. 2019; Tóth et al. 2008) warrants increased research into *P. teres* f. *maculata.*

1.2. Life cycle

P. teres f. *teres* and *P. teres* f. *maculata* share similar life cycles. As a stubble-borne pathogen, *P. teres* over-winters on barley debris by producing a protective ascocarp structure in the form of pseudothecia. Heterothallic in nature, sexual reproduction of *P. teres* requires two genetically distinct mating types (Rau et al. 2005). In the presence of compatible mating types, pseudothecia develop asci, which usually then produce eight ascospores each (Kenneth 1962). These ascospores can be dispersed by wind or rain and land on barley foliage at any growth stage, where the colonization process may begin (Jordan 1981). Conidia and mycelia left on infected stubble may also serve as primary inoculum if dispersed (Jordan and Allen 1984; McLean et al. 2009). Following primary inoculation, *P. teres* produces additional clonal conidia throughout the growing season. This secondary inoculum can be further dispersed by wind and rain, allowing the disease to spread within fields and into previously unaffected regions (Jordan 1981; Mathre 1997). Under warm and humid conditions, *P. teres* can colonize leaf tissue and sporulate in as little as five days, allowing for many disease cycles throughout the growing season (Jordan 1981).

1.3. Disease control

Strategies used to control the spread and severity of net form and spot form net blotch include cultural practices, fungicide use, and breeding for resistance (Liu et al. 2011). Cultural practices may consist of crop rotation, burying of stubble, and adequate watering and fertilization. Crop rotation and avoidance of barley monocultures, as well as burying or burning of stubble may prevent *P. teres* from becoming established in a field or minimize its prominence

(Liu et al. 2011; Jordan and Allen 1984). It has been suggested that a period of two or more years between successive barley crops is necessary to prevent reinfection from contaminated stubble (Duczek et al. 1999). Adequate watering and fertilization promote overall plant health, including disease resistance, though fertilizing with excess nitrogen may increase NFNB disease severity (Kangor et al. 2017). Fungicides such as quinone outside inhibitors, demethylation inhibitors, and succinate dehydrogenase inhibitors have been shown to inhibit the growth of *P. teres*, though instances of resistance to these fungicides have been noted (Mair et al. 2016; Ellwood et al. 2019; Rehfus et al. 2017). Due to the uncertainty of disease avoidance via cultural practices as well as the environmental risks associated with fungicide use, breeding of resistant crops remains an attractive and economical option.

1.4. Mechanics of pathogen virulence

P. teres spores may begin germinating within hours of initially landing on a barley leaf under sufficient and sustained humidity (van den Berg and Rossnagel 1990). During the process of germination, spores produce germ tubes that can extend up to 0.5 cm before developing appressoria. These structures can then produce penetration pegs, which are used to gain access into epidermal cells (Van Caeseele and Grumbles 1979). Primary and secondary intracellular infection vesicles then develop, disrupting the activity of these and adjacent epidermal cells. Subsequent growth from these vesicles extends intercellularly into the mesophyll, where the function of nearby cells can also be negatively affected (Keon and Hargreaves 1983). This disruption can result in cell death in susceptible reactions. Along with the brown necrotic lesions that are indicative of *P. teres*, regions of chlorosis commonly develop in the leaf during the infection process. Chlorosis is the result of disruption or destruction of the cellular chloroplasts, resulting in yellow-white areas on the leaf where photosynthesis can no longer occur. Electron

microscopy of these regions has shown that fungal hyphae do not have to be present for chlorosis to occur, suggesting factors secreted ahead of the pathogen may be the cause of this disruption (Keon and Hargreaves 1983). Phytotoxic proteinaceous metabolites have been shown to contribute to the development of similar chlorotic symptoms, though an association with disease is tenuous (Sarpeleh et al. 2007; 2008; 2009).

Differences in infection characteristics have been observed between *P. teres* f. *teres* and *P. teres* f. *maculata*, including variations in time to germination and degree of hyphal extension prior to appressorium formation (Lightfoot and Able 2010). After initial formation of intracellular vesicles and entrance into the mesophyll, *P. teres* f. *teres* has been observed to extend hyphae more so along a horizontal plane relative to the point of penetration, whereas *P. teres* f. *maculata* appears to grow more significantly perpendicular to the leaf surface (Lightfoot and Able 2010). Additionally, variations in rate of growth *in planta* have been observed within an assemblage of *P. teres* isolates collected in Israel, with *P. teres* f. *maculata* displaying a 70% higher rate of growth over *P. teres* f. *teres* (Ronen et al. 2019). Variations in the rate of germination and appressorium formation among *P. teres* f. *teres* isolates have also been suggested to correlate with virulence (Ismail et al. 2014a).

1.5. Genomics

The first *P. teres* genome assembly was of the Canadian *P. teres* f. *teres* isolate 0-1, made using 75 bp paired-end Illumina reads and resulting in a predicted total genome size of 41.95 Mbp at 20× coverage (Ellwood et al. 2010). However, due to roughly 95% of the initial contigs being less than 200 bp, it was likely that highly repetitive stretches of DNA were lost – an inherent limitation of short read assemblies (Alkan et al. 2011). To better capture repetitive genomic regions and further characterize the *P. teres* f. *teres* genome, Pacific Biosciences long-

read sequencing was used by Wyatt et al. (2018) to create a high-quality reference assembly of isolate 0-1. This assembly used an average read length of 8051 bp and achieved an average coverage of 200×. After scaffolding with linkage maps generated from *P. teres* f. *teres* biparental populations, the assembly resulted in a total genome size of roughly 46.5 Mbp, 91.8% of which was distributed across 12 scaffolds. This suggested that 12 chromosomes comprise the *P. teres* f. *teres* genome, as compared to the nine observed previously via cytological karyotyping (Ellwood et al. 2010).

The first *P. teres* f. *maculata* reference genome was published by Syme et al. (2018). This study compared the genomes of two *P. teres* f. *maculata* isolates and five *P. teres* f. *teres* isolates using long-read sequencing, genetic mapping, and optical mapping. Genome assemblies of 39.27-41.28 Mbp for the *P. teres* f. *maculata* isolates and 46.31-51.76 Mbp for the *P. teres* f. *teres* isolates were obtained, indicating a genome size discrepancy between the two forms. To date, there are 11 publicly available *P. teres* f. *teres* total genome sequence assemblies and five total *P. teres* f. *maculata* genome assemblies (Moolhuijzen et al. 2020; Wyatt et al. 2020; Wyatt and Friesen 2021). Expansion in repetitive elements is almost completely responsible for the larger *P. teres* f. *teres* genome as inferred from variation in the non-GC equilibrated (AT-rich) genomic fraction (Syme et al. 2018). While the gene-dense regions of the two forms share a high degree of synteny, repetitive AT-rich regions in *P. teres* f. *teres* are more numerous and generally greater in length relative to *P. teres* f. *maculata* (Syme et al. 2018).

Both forms of *P. teres* demonstrate the "two-speed" genomic architecture characteristic of filamentous plant pathogens, i.e., relatively stable, gene-rich core compartments alongside dynamic, gene-sparse, repetitive regions often overrepresented in transposable elements (TEs) and effector proteins (Dong et al. 2015; Möller and Stukenbrock 2017; Faino et al. 2016). This is

exemplified by Wyatt et al. (2020), who compared the genomes of five *P. teres* f. *teres* isolates to investigate the attributes of annotated genes within these dynamic regions, termed the accessory genome. Accessory genomic compartments often fell within subtelomeric regions and were shown to harbor higher rates of single nucleotide polymorphisms (SNPs) along with higher rates of nonsynonymous SNPs in comparison with genomic regions shared between all isolates. Additionally, these accessory regions feature significantly higher rates of TE insertions, shorter proteins, and a greater abundance of proteins lacking conserved domains. Analysis of prior quantitative trait loci (QTL) studies (Koladia et al. 2017; Lai et al. 2007; Shjerve et al. 2014) indicate that most of the *P. teres* f. *teres* loci associated with virulence lie within these subtelomeric accessory regions.

1.6. Effectors

Effectors include any factors secreted by a pathogen to manipulate host physiology and accommodate colonization. Fungal effectors can include proteins, toxic secondary metabolites, or small RNAs (Franceshetti et al. 2017; Collemare et al. 2019). To date, most research into fungal effectors has focused on proteins. Effectors of biotrophic pathogens often function to avoid recognition by the host (Reviewed in Lo Presti et al. 2015), whereas necrotrophic effectors are generally used to hijack the host defense response, resulting in programmed cell death and host susceptibility (Reviewed in Friesen and Faris 2021). It is likely that *P. teres* secretes both biotrophic and necrotrophic effectors during the infection cycle, as there is an asymptomatic period of intracellular growth and nutrient acquisition prior to the development of necrosis (Lightfoot et al. 2017).

AvrHar was the first identified genomic locus in *P. teres* to be associated with virulence (Weiland et al. 1999). Discovered by crossing the Canadian *P. teres* f. *teres* isolate 0-1 with the

Californian isolate 15A, this locus appeared to confer avirulence on the barley line Harbin. Subsequent research indicated the involvement of this same locus with avirulence on lines Tifang and Canadian Lake Shore (Lai et al. 2007), with 15A contributing the avirulent allele in both instances. Lai et al. (2007) also identified two genes contributed by 0-1 that conferred virulence on line Prato, designated as *AvrPra1* and *AvrPra2*. Interestingly, *AvrPra2* was shown to co-segregate with *AvrHar*, implying that allelic forms of the same gene or two closely linked genes may be associated with both virulence and avirulence, depending on the host line. In a mapping population created by mating Canadian *P. teres* f. *teres* isolates WRS 1906 and WRS 1607, Beattie et al. (2007) identified the gene $Avr_{Heartland}$ as being associated with avirulence on the barley cultivar Heartland.

In contrast to previously mentioned studies that relied on random amplification techniques to find genomic polymorphisms, Shjerve et al. (2014) was the first to use genotyping by sequencing, a more efficient process for creating genetic maps, to identify these differences in *P. teres* f. *teres*. Using this approach with a 15A × 6A population, four unique QTL were mapped – *VK1* and *VK2* contributed by *P. teres* f. *teres* isolate 15A and conferring virulence on line Kombar, and *VR1* and *VR2* contributed by *P. teres* f. *teres* isolate 6A and conferring virulence on line Rika. Progeny isolates harboring only *VK1*, *VK2*, or *VR2* were inoculated on a Rika × Kombar mapping population to map host-side susceptibility loci, resulting in the identification of a single susceptibility locus on chromosome 6H. This genotyping by sequencing approach was also used to find QTL associated with virulence in a biparental mapping population derived from the Danish *P. teres* f. *teres* isolate BB25 and the North Dakotan *P. teres* f. *teres* isolate FGOH04Ptt-21 (Koladia et al. 2017). This population was inoculated on a panel

of eight diverse barley lines resulting in nine unique QTL, of which three contributed half or more of the phenotypic variation for a specific line.

A GWAS of 188 Australian *P. teres* f. *teres* isolates that had been phenotyped across 20 different barley genotypes found 14 genomic regions associated with virulence (Martin et al. 2020). The same group then performed QTL mapping using two different biparental populations and confirmed an association with virulence in four of these regions. By comparing the 14 genomic regions to the W1-1 *P. teres* f. *teres* reference genome, 20 candidate effectors were identified, of which one was a previously characterized secreted protein associated with virulence (Ismail and Able 2017).

Proteomic approaches have shown varying levels of success in identifying effector proteins as compared to marker trait association studies. The proteinaceous necrotrophic effector PttNE1 was isolated by Liu et al. (2015) from intercellular wash fluids of barley line Hector inoculated with isolate 0-1. This protein was shown to interact with a susceptibility gene designated as *SPN1*, which was mapped to a region of barley chromosome 6H commonly identified as associating with resistance/susceptibility (Reviewed in Clare et al. 2020). Three proteins differentially expressed between *P. teres* f. *teres* isolates with contrasting virulence patterns were identified via 2-D gel electrophoresis of culture filtrates and shown to have homology to other proteins broadly involved in plant-pathogen interactions (Ismail et al. 2014b). Subsequent proteomic studies have identified proteins common to virulent *P. teres* f. *teres* isolates from culture filtrates and looked at the expression *in planta* of such proteins (Ismail and Able 2016; 2017).

To date, there has only been one study mapping virulence in *P. teres* f. *maculata*. Carlsen et al. (2015) crossed *P. teres* f. *maculata* isolates FGOB10Ptm-1 and SG1 and inoculated the

progeny of the cross on a commonly used SFNB differential set composed of four barley lines, resulting in the identification of eight QTL associated with virulence. One virulence locus was contributed by SG1 and seven were contributed by FGOB10Ptm-1, though three of these were present in a closely linked region. While the QTL in this closely linked region may be representative of several individual genes, it is likely that a single shared gene is contributing this virulence (Carlsen et al. 2015).

1.7. *P. teres* on wheat

Emerging pathogens can be classified as any pathogen that has become the causal agent of a new disease or displayed increased incidence of disease, expanded its geographic range, displayed alterations in pathogenicity, or caused disease on a novel host (Anderson et al. 2004; Fones et al. 2020). The most common causes of disease emergence are introduction of a pathogen to a previously unaffected area via human activity and severe weather events, with many of these events shown to be influenced by a rapidly changing climate (Anderson et al. 2004; Bebber and Gurr 2015; Rosenzweig et al. 2001). Although its primary host is barley, *P. teres* has been observed on a range of related gramineous species as a result of both natural infection and artificial inoculations (Reviewed in Liu et al. 2011). First reports of *P. teres* f. *maculata* causing disease on wheat have come out of Hungary (Tóth et al. 2008) and Russia (Mikhailova et al. 2010), with the pathogen most recently isolated from wheat leaves in Argentina (Perelló et al. 2019).

Two of the Argentinian isolates, PT2047 and PT2050, were inoculated on a geographically diverse set of spring wheat genotypes (Uranga et al. 2020). Subsequent marker-trait analysis identified nine markers associated with resistance to *P. teres* f. *maculata*. Three of these markers had not before been associated with disease resistance, while four others had

previously been reported as being associated with resistance to tan spot, the disease caused by the closely related wheat pathogen *Pyrenophora tritici-repentis* (Uranga et al. 2020). Field and pot inoculations of the same two Argentinian *P. teres* f. *maculata* isolates were then performed alongside *P. tritici-repentis* isolate PtrH017 on a set of 30 commercially planted Argentinian wheat cultivars for comparative resistance screening (Uranga 2021). A variety of disease responses were observed across the panel, with marked differences in resistance/susceptibility in several cultivars observed between the two *Pyrenophora* species.

1.8. Literature cited

Alkan, C., Sajjadian, S., and Eichler, E. E. 2011. Limitations of next-generation genome sequence assembly. Nat. Methods. 8:61-65.

Anderson, P. K., Cunningham, A. A., Patel, N. G., Morales, F.J., Epstein, P. R., and Daszak, P. 2004. Emerging infectious diseases of plants: Pathogen pollution, climate change and agrotechnology drivers. Trends Ecol. Evol. 19:535-544.

Atanasoff, D. and Johnson, A.G. 1920. Treatment of cereal seeds by dry heat. J. Agric. Res. 18:379-390.

Beattie, A. D., Scoles, G. J., and Rossnagel, B. G. 2007. Identification of molecular markers linked to a *Pyrenophora teres* avirulence gene. Phytopathology. 97:842-849.

Bebber, D. P., and Gurr, S. J. 2015. Crop-destroying fungal and oomycete pathogens challenge food security. Fungal Genet. Biol. 74:62-64.

Carlsen, S. A., Neupane, A., Wyatt, N. A., Richards, J. K., Faris, J. D., Xu, S. S., Brueggeman, R. S., and Friesen, T. L. 2015. Characterizing the *Pyrenophora teres* f. *maculata*-barley interaction using pathogen genetics. G3-Genes Genom. Genet. 7:2615-2626.

Clare, S. J., Wyatt, N. A., Brueggeman, R. S., and Friesen, T. L. 2020. Research advances in the *Pyrenophora teres*-barley interaction. Mol. Plant Pathol. 21:272-288.

Collemare, J., O'Connell, R., and Lebrun, M. H. 2019. Nonproteinaceous effectors: The terra incognita of plant-fungal interactions. New Phytol. 223:590-596.

Dong, S., Raffaele, S., and Kamoun, S. 2015. The two-speed genomes of filamentous pathogens: Waltz with plants. Curr. Opin. Genet. Dev. 35:57-65.

Duczek, L. J., Sutherland, K. A., Reed, S. L., Bailey, K. L., and Lafond, G. P. 1999. Survival of leaf spot pathogens on crop residues of wheat and barley in Saskatchewan. Can. J. Plant. Pathol. 21:165-173.

Ellwood, S. R., Liu, Z., Syme, R. A., Lai, Z., Hane, J. K., Keiper, F., Moffat, C. S., Oliver, R. P., and Friesen, T. L. 2010. A first genome assembly of the barley fungal pathogen *Pyrenophora teres* f. *teres*. Genome Biol. 11:11.

Ellwood, S. R., Piscetek, V., Mair, W. J., Lawrence, J. A., Lopez-Ruiz, F. J. and Rawlinson, C. 2019. Genetic variation of *Pyrenophora teres* f. *teres* isolates in Western Australia and emergence of a Cyp51A fungicide resistance mutation. Plant Pathol. 68:135-142.

Faino, L., Seidl, M. F., Shi-Kunne, X., Pauper, M., van den Berg, G. C., Wittenberg, A. H., and Thomma, B. P. H. J. 2016. Transposons passively and actively contribute to evolution of the two-speed genome of a fungal pathogen. Genome Res. 26:1091-1100.

Fones, H. N., Bebber, D. P., Chaloner, T. M., Kay, W. T., Steinberg, G., and Gurr, S. J. 2020. Threats to global food security from emerging fungal and oomycete crop pathogens. Nat. Food. 1:332-342.

Franceschetti, M., Maqbool, A., Jiménez-Dalmaroni, M. J., Pennington, H. G., Kamoun, S., and Banfield, M. J. 2017. Effectors of filamentous plant pathogens: Commonalities amid diversity. Microbiol. Mol. Biol. R. 81:2.

Friesen T. L., and Faris, J. D. 2021. Characterization of effector-target interactions in necrotrophic pathosystems reveals trends and variation in host manipulation. Annu. Rev. Phytopathol. 59:4.1-4.22.

Ismail, I. A., and Able, A. J. 2016. Secretome analysis of virulent *Pyrenophora teres* f. *teres* isolates. Proteomics. 16:2625-2636.

Ismail, I. A., and Able, A. J. 2017. Gene expression profiling of virulence-associated proteins *in planta* during net blotch disease of barley. Physiol. Mol. Plant P. 98:69-79.

Ismail, I. A., Godfrey, D., and Able, A. J. 2014a. Fungal growth, proteinaceous toxins and virulence of *Pyrenophora teres* f. *teres* on barley. Australas. Plant Path. 43:535-546.

Ismail, I. A., Godfrey, D., and Able, A. J. 2014b. Proteomic analysis reveals the potential involvement of xylanase from *Pyrenophora teres* f. *teres* in net form net blotch disease of barley. Australas. Plant Path. 43:715-726.

Jordan, V. W. L. 1981. Aetiology of barley net blotch caused by *Pyrenophora teres* and some effects on yield. Plant Pathol. 30:77-87.

Jordan, V. W. L., and Allen, E. C. 1984. Barley net blotch: Influence of straw disposal and cultivation methods on inoculum potential, and on incidence and severity of autumn disease. Plant Pathol. 33:547-559.

Kangor, T., Sooväli, P., Tamm, Y., Tamm, I., and Koppel, M. 2017. Malting barley diseases, yield and quality – responses to using various agro-technology regimes. Proc. Latv. Acad. Sci. B: Nat. Exact Appl. Sci. 711:57-62.

Kenneth, R. 1962. On the taxonomy, morphology and geographical origins of *Pyrenophora teres* Drechsler and allied species. Bull. Res. Council Israel. 11:55-82.

Keon, J. P. R., and Hargreaves, J. A. 1983. A cytological study of the net blotch disease of barley caused by *Pyrenophora teres*. Physiol. Plant Pathol. 22:321-329.

Khan, T. N. 1982. Changes in pathogenicity of *Drechslera teres* relating to changes in barley cultivars grown in Western Australia. Plant Dis. 66:655-656.

Khan, T. N. and Boyd, W. J. R. 1969. Inheritance of resistance to net blotch in barley. II. Genes conditioning resistance against race W.A.-2. Can. J. Genet. Cytol. 11:592-597.

Koladia, V. M., Richards, J. K., Wyatt, N. A., Faris, J. D., Brueggeman, R. S., and Friesen, T. L. 2017. Genetic analysis of virulence in the *Pyrenophora teres* f. *teres* population BB25 ×FGOH04Ptt-21. Fungal Genet. Biol. 107:12-19.

Lai, Z., Faris, J. D., Weiland, J. J., Steffenson, B., and Friesen, T. L. 2007. Genetic mapping of *Pyrenophora teres* f. *teres* genes conferring avirulence on barley. Fungal Genet. Biol. 44:323-329.

Lightfoot, D. J., Able, A. J. 2010. Growth of *Pyrenophora teres* in planta during barley net blotch disease. Australas. Plant Path. 39:499-507.

Lightfoot, D. J., Mcgrann, G. R. D., and Able, A. J. 2017. The role of a cytosolic superoxide dismutase in barley-pathogen interactions. Mol. Plant Pathol. 18:323-335.

Liu, Z. H., and Friesen, T. L. 2010. Identification of *Pyrenophora teres* f. *maculata*, causal agent of spot type net blotch of barley in North Dakota. Plant Dis. 94:480.

Liu, Z., Ellwood, S. R., Oliver, R. P., and Friesen, T. L. 2011. *Pyrenophora teres*: Profile of an increasingly damaging barley pathogen. Mol. Plant Pathol. 121:1-19.

Liu, Z., Holmes, D. J., Faris, J. D., Chao, S., Brueggeman, R. S., Edwards, M. C., and Friesen, T. L. 2015. Necrotrophic effector-triggered susceptibility (NETS) underlies the barley-*Pyrenophora teres* f. *teres* interaction specific to chromosome 6H. Mol. Plant Pathol. 16:188-200.

Lo Presti, L., Lanver, D., Schweizer, G., Tanaka, S., Liang, L., Tollot, M., Zuccaro, A., Reissmann, S., and Kahmann, R. 2015. Fungal effectors and plant susceptibility. Annu. Rev. Plant Biol. 66:513-545.

Louw, J. P., Crous, P. W., and Holz, G. 1996. Relative importance of the barley net blotch pathogens *Pyrenophora teres* f. *teres* (net type) and *P. teres* f. *maculata* (spot type) in South Africa. Afr. Plant Prot. 2:89-95.

Mair, W. J., Deng, W., Mullins, J. G., West, S., Wang, P., Besharat, N. Ellwood, S. R., Oliver, R. P., and Lopez-Ruiz, F. J. 2016. Demethylase inhibitor fungicide resistance in

Pyrenophora teres f. sp. *teres* associated with target site modification and inducible overexpression of *Cyp51*. Front Microbiol. 7:1279.

Marshall, J. M., Kinzer, K., and Brueggeman, R. S. 2015. First report of *Pyrenophora teres* f. *maculata* the cause of spot form net blotch of barley in Idaho. Plant Dis. 99:1860.

Martin, A., Moolhuijzen, P., Tao, Y., McIlroy, J., Ellwood, S., Fowler, R., Platz, G. J., Kilian, A., and Snyman, L. 2020. Genomic regions associated with virulence in *Pyrenophora teres* f. *teres* identified by genome-wide association analysis and biparental mapping. Phytopathology. 110:881-891.

Mathre, D.E. 1997. *Compendium of Barley Diseases, 2nd edn*. St. Paul, MN: American Phytopathological Society.

McLean, M. S., Howlett, B. J., and Hollaway, G. J. 2009. Epidemiology and control of spot form of net blotch *Pyrenophora teres* f. *maculata* of barley: A review. Crop Pasture Sci. 60:303-315.

McLean, M. S., Howlett, B. J., and Hollaway, G. J. 2010. Spot form of net blotch, caused by *Pyrenophora teres* f. *maculata,* is the most prevalent foliar disease in Victoria, Australia. Australas. Plant Path. 39:46-49.

Mikhailova, L.A., Ternyuk, I.G., and Mironenko, N.V. 2010. *Pyrenophora teres*, an agent causing wheat leaf spot. Microbiology. 79:561-565.

Möller, M., and Stukenbrock, E. 2017. Evolution and genome architecture in fungal plant pathogens. Nat. Rev. Microbiol. 15:756-771.

Moolhuijzen, P. M., Muria-Gonzalez, M. J., Syme, R., Rawlinson, C., See, P. T., Moffat, C. S., and Ellwood, S. R. 2020. Expansion and conservation of biosynthetic gene clusters in pathogenic *Pyrenophora* spp. Toxins. 12:242.

Perelló, A. E., Couretot, L., Curti, A., Uranga, J. P. and Consolo, V. F. 2019. First report of spot lesion of wheat caused by *Pyrenophora teres* f. sp *maculata* observed in Argentina. Crop Prot. 122:19-22.

Rau, D., Maier, F. J., Papa, R., Brown, A. H. D., Balmas, V., Saba, E., Schaefer, W., and Attene, G. 2005. Isolation and characterization of the mating-type locus of the barley pathogen *Pyrenophora teres* and frequencies of mating-type idiomorphs within and among fungal populations collected from barley landraces. Genome. 48:855-869.

Rehfus, A., Strobel, D., Bryson, B., and Stammler, G. 2017. *Sensitivity of Pyrenophora teres to succinate dehydrogenase inhibitors in Europe. Modern Fungicides and Antifungal Compounds. Vol. VIII.* Braunschweig: 175-180.

Ronen, M., Sela, H., Fridman, E., Perl-Treves, R., Kopahnke, D., Moreau, A. Ben-David, R., and Harel, A. 2019. Characterization of the barley net blotch pathosystem at the center of origin of host and pathogen. Pathogens. 8:275.

Rosenzweig, C., Iglesius, A., Yang, X. B., Epstein, P. R., and Chivian, E. 2001. Climate change and extreme weather events – Implications for food production, plant diseases, and pests. Global Change and Human Health. 2:90-104.

Sarpeleh, A., Tate, M. E., Wallwork, H., Catcheside, D., and Able, A. J. 2009. Characterisation of low molecular weight phytotoxins isolated from *Pyrenophora teres*. Physiol. Mol. Plant P. 73:154-162.

Sarpeleh, A., Wallwork, H., Catcheside, D. E. A., Tate, M.E., and Able, A. J. 2007. Evidence of involvement of proteinaceous toxins from *Pyrenophora teres* in symptom development of net blotch of barley. Phytopathology. 97:907-915.

Sarpeleh, A., Wallwork, H., Tate, M.E., Catcheside, D. E. A., and Able, A. J. 2008. Initial characterization of phytotoxic proteins isolated from *Pyrenophora teres*. Physiol. Mol. Plant P. 72:73-79.

Shipton, W. A., Khan, T. N., and Boyd, W. J. R. 1973. Net blotch of barley. Rev. Plant Pathol. 52:269-290.

Shjerve, R. A., Faris, J. D., Brueggeman, R. S., Yan, C., Zhu, Y., Koladia, V., and Friesen, T. L. 2014. Evaluation of a *Pyrenophora teres* f. *teres* mapping population reveals multiple independent interactions with a region of barley chromosome 6H. Fungal Genet. Biol. 70:104-112.

Smedegård-Petersen, V. 1971. *Pyrenophora teres f. maculata f. nov. and Pyrenophora teres f. teres on barley in Denmark.* Copenhagen: Yearbook of the Royal Veterinary and Agricultural University. 124-144.

Syme, R. A., Martin, A., Wyatt, N. A., Lawrence, J. A., Muria-Gonzalez, M. J., Friesen, T. L., and Ellwood, S. R. 2018. Transposable element genomic fissuring in *Pyrenophora teres* is associated with genome expansion and dynamics of host-pathogen genetic interactions. Front. Gen. 9:130.

Tekauz, A. 1985. A numerical scale to classify reactions of barley to *Pyrenophora teres*, Can. J. Plant Pathol. 7:181-183.

Tóth, B., Csősz, M., Kopahnke, D. and Varga, J. 2008. First report on *Pyrenophora teres* causing lesions of wheat leaves in Hungary. Plant Pathol. 57.

Uranga, J. P., Perelló, A. E., Schierenbeck, M., and Simón, M. R. 2021. First screening for resistance in Argentinian cultivars against *Pyrenophora teres F. maculata*, a recently reported pathogen in wheat. Eur. J. Plant Pathol. 161:357-369.

Uranga, J. P., Schierenbeck, M., Perelló, A. E., Lohwasser, U., Börner, A., and Simón, M. R. 2020. Localization of QTL for resistance to *Pyrenophora teres f. maculata*, a new wheat pathogen. Euphytica. 216:56.

van Caeseele, L., and Grumbles, J. 1979. Ultrastructure of the interaction between *Pyrenophora teres* and a susceptible barley host. Can. J. Bot. 57:40-47.

van den Berg, C. G. J., and Rossnagel, B. G. 1990. Effects of temperature and leaf wetness period on conidium germination and infection of barley by *Pyrenophora teres*. Can. J. Plant Pathol. 12:263-266.

Weiland, J. J., Steffenson, B. J., Cartwright, R. D., and Webster, R. K. 1999. Identification of molecular genetic markers in *Pyrenophora teres* f. *teres* associated with low virulence on 'Harbin' barley. Phytopathology. 89:176-181.

Wyatt and Friesen 2021. Four reference quality genome assemblies of *Pyrenophora teres* f. *maculata*: A resource for studying the barley spot form net blotch interaction. Mol. Plant-Microbe Interact. 34:135-139.

Wyatt, N. A., Richards, J. K., Brueggeman, R. S., and Friesen, T. L. 2018. Reference assembly and annotation of the *Pyrenophora teres* f. *teres* isolate 0-1. G3-Genes Genom. Genet. 8:1-8.

Wyatt, N. A., Richards, J. K., Brueggeman, R. S., and Friesen, T. L. 2020. A comparative genomic analysis of the barley pathogen *Pyrenophora teres* f. *teres* identifies subtelomeric regions as drivers of virulence. Mol. Plant-Microbe Interact. 33:173-188.

CHAPTER 2. VALIDATION OF *P. TERES* F. *TERES PTTBEE1* EFFECTOR CANDIDATES

2.1. Abstract

Net from net blotch (NFNB), is a significant foliar disease of barley caused by the fungal pathogen *Pyrenophora teres* f. *teres*. This pathogen is present in all barley-growing regions worldwide and can cause substantial crop losses under conducive environmental conditions. As a heterothallic fungus, *P. teres* f. *teres* can rapidly evolve its effector repertoire, leading to high virulence diversity among isolates. Identification of effectors contributing to virulence is essential for characterizing the interaction between host and pathogen and for providing the knowledge necessary to generate barley cultivars with durable resistance. Eight candidate effector genes were identified at the *P. teres* f. *teres PttBee1* locus based on polymorphisms between parents and characteristics commonly associated with effectors. The role these candidates may play in virulence on Beecher barley was assessed using gain-of-function transformations and CRISPR-Cas9 mediated gene disruptions. As no change in phenotype was observed after manipulating these genes, new genomic markers were designed to provide additional mapping power at the *PttBee1* quantitative trait locus (QTL), resulting in an increase in the LOD value and significance of the QTL. The data presented here show that further research is necessary to identify the effector underlying *PttBee1*, and that implementation of new markers was effective for refining the location of *PttBee1*.

2.2. Introduction

Pyrenophora teres f. *teres* is the causative agent of the barley foliar disease NFNB. Barley leaves affected by NFNB display characteristic necrotic lesions on the surface of the leaf, often accompanied by regions of chlorosis (Shipton et al. 1973). Under favorable conditions,

compatible interactions can result in total leaf death, culminating in decreased grain yield and quality (Mathre 1997). Though the spread and severity of disease caused by *P. teres* f. *teres* can be partially mitigated through the application of fungicides and the burying or burning of barley stubble, use of resistant cultivars is the preferred method for combatting this pathogen.

Identification and selection of resistant barley genotypes can be facilitated by research into the molecular mechanisms underlying pathogen virulence. Diversity in *P. teres* f. *teres* virulence was first documented by Khan and Boyd (1969), who observed three distinct Australian races on two different barley lines. Subsequent screening of globally collected isolates against diverse barley differential lines has revealed a wide range of virulence profiles (Reviewed in Liu et al. 2011). Quantitative trait loci (QTL) analysis of pathogen mapping populations as well as genome wide association studies (GWAS) can be used to identify specific genomic regions associated with virulence/avirulence, a necessary step in further characterizing the virulence profile of *P. teres* f. *teres*.

Beginning with the initial identification of the *AvrHar* locus by Weiland et al. (1999), marker trait association studies such as QTL analysis and GWAS have resulted in the discovery of loci associated with virulence on nearly all *P. teres* f. *teres* chromosomes, often located within subtelomeric regions (Reviewed in Clare et al. 2020; Martin et al. 2020; Wyatt et al. 2020). Additional methods that have been used to identify genes or proteins associated with virulence include 2-D gel electrophoresis of culture filtrates and gene expression profiling via qPCR (Ismail and Able 2016; 2017). Liu et al. (2015) identified a *P. teres* f. *teres* protein responsible for conferring virulence on barley line Hector. Isolated from intercellular wash fluids of Hector inoculated with *P. teres* f. *teres* isolate 0-1, the proteinaceous effector PttNE1 was shown to interact with the barley resistance/susceptibility locus *SPN1*, accounting for 31% of the disease

variation when 0-1 was inoculated on a barley mapping population (Liu et al. 2015). Though the gene encoding this protein is yet to be identified, this study provided evidence that the *P. teres* f. *teres*-barley pathosystem in some measure follows a necrotrophic effector-triggered susceptibility (NETS) model.

Effectors can include any factors secreted by a pathogen that serve to manipulate host physiology to accommodate colonization, often by preventing recognition of the pathogen or by hijacking the host defense response (Reviewed in Friesen and Faris 2021; Reviewed in Lo Presti et al. 2015). Though fungal effectors vary greatly in amino acid sequence and protein structure, they often share characteristics such as the presence of a secretion signal, high cysteine content, lack of transmembrane domains and cell-surface anchors, and small size (Franceschetti et al. 2017). The identification of effector candidates has been accelerated using bioinformatic tools designed to detect or predict these characteristics, allowing for the generation of candidate lists using genomic and transcriptomic data (Reviewed in Jones et al. 2018).

Our lab previously identified nine QTL associated with virulence across four NFNB differential lines and four local cultivars using a *P. teres* f. *teres* biparental mapping population (Koladia et al. 2017). A QTL associated with 56% of the variation in virulence on Beecher barley was identified and designated as *PttBee1*. In the current study, effector candidates within the *PttBee1* region were identified and manipulated to evaluate their involvement in virulence, and new markers were developed and mapped to refine the *PttBee1* QTL.

2.3. Materials and methods

2.3.1. Candidate selection and annotation analysis

Effector candidates were selected based on the criteria described by Wyatt et al. (2020). Briefly, the genomic region encompassed by the *PttBee1* QTL for both *P. teres* f. *teres* isolates

BB25 and FGOH04Ptt-21 (FGO21) were screened for annotated gene models produced by the Maker2 pipeline (Holt and Yandell 2011) in conjunction with RNA sequencing data (Wyatt et al. 2020). Potentially secreted genes were identified using SignalP v5.0 (Almagro Armenteros et al. 2019), Deeploc v1.0 (Almagro Armenteros et al. 2017), and SecretomeP v2.0 (Bendtsen et al. 2004). Transmembrane domains were predicted using TMHMM v2.0 (Krogh et al. 2001). Glycosylphosphatidylinositol (GPI) cell-surface anchors were predicted using NetGPI v1.1 (Gíslason et al. 2021). Initial effector candidates were identified using EffectorP v2.0 (Sperschneider et al. 2018). Protein functional domains were predicted using Interproscan v5.52-86.0 (Jones et al. 2014). Gene models were visualized and compared using Geneious Prime® 2021.1.1 (https://www.geneious.com). Geneious functions "Blastn", "Blastp", and "Megablast" were used to identify unique or homologous genes between genomes. The "Geneious Alignment" function was used to compare DNA and amino acid sequences.

2.3.2. Oligonucleotide design

General primers for gene amplification were designed using Primer3 v4.1.0 (Untergasser et al. 2012). Primers for amplification of PCR products to be used as substrates in the Gateway® cloning process were designed as described in the Gateway® Technology User Guide (Invitrogen, https://tools.thermofisher.com/content/sfs/manuals/gatewayman.pdf). Briefly, forward primers were designed to contain, in the 5'-3' direction, four guanine residues followed by the 25 bp *att*B1 site, preceding an 18 to 25 bp sequence homologous to a region upstream of the native promoter of the effector candidate gene. Likewise, reverse primers were designed to contain, in the 5'-3' direction, four guanine residues followed by the 25 bp *att*B2 site, preceding the reverse-complement of the 18 to 25 bp sequence containing the stop codon of the effector candidate gene. For use in CRISPR-Cas9 mediated gene disruptions, a DNA primer for sgRNA

synthesis was designed using E-CRISP v5.4 (Heigwer et al. 2014). The closely related *Zymoseptoria tritici* MG2.31 was chosen as the reference genome, and the application was run using "strict" or "medium" stringencies. For amplification of donor DNA to be used in CRISPR-Cas9 gene disruptions, forward primers were designed to contain a 40 bp homologous sequence 3 bp upstream of the respective protospacer adjacent motif (PAM) site, based on the E-CRISP output, followed by a 16 bp M13F primer for amplification of a hygromycin resistance cassette. Reverse primers were designed similarly, with the 17 bp M13R primer followed by the reverse-complement of the 40 bp immediately following the respective PAM site. All primers were screened against the respective *P. teres* f. *teres* genomes using the Geneious "Blastn" function to identify possible off-target homology.

2.3.3. sgRNA synthesis and RNP formation

sgRNAs were synthesized and complexed with Cas9-NLS immediately preceding fungal transformations. sgRNA was synthesized using the EnGen® sgRNA Synthesis Kit (New England Biolabs, Inc.). Briefly, the sgRNA DNA primers were combined with nuclease-free water, EnGen 2X sgRNA reaction mix, *S. pyogenes*, and EnGen sgRNA enzyme mix, followed by a 30 min incubation at 37 °C. DNase I and additional nuclease-free water were added to these reactions followed by incubation at 37 °C for 15 min. The resulting sgRNAs were purified using the Zymo RNA Clean & Concentrator™-5 kit (Zymo Research). Briefly, sgRNAs were combined with RNA binding buffer and 100% ethanol, followed by centrifugation through Zymo-Spin™ IC columns to capture RNA. Additional centrifugation steps were performed following the addition of RNA prep buffer and RNA wash buffer to remove impurities before eluting with DNase/Rnase-free water and quantification. 2 µg sgRNA was placed on ice for immediate complexing with Cas9-NLS protein, with excess sgRNA stored at -80 °C. To form

sgRNA-Cas9-NLS complexes, sgRNAs were combined with EnGen® Spy Cas9 NLS (New England Biolabs, Inc.), EnGen® Cas9-NLS Buffer, and nuclease-free water, and then incubated for 15 min at 25 °C. Complexed sgRNA-Cas9-NLS was stored on ice prior to transformation.

2.3.4. Construction of fungal gain-of-function transformation vectors

Identified candidate genes, including a region of ~1000 bp upstream to preserve the native promoter region, were amplified using high-fidelity polymerase from genomic DNA with primers designed with *att*B1 and *att*B2 sequences. PCR products were loaded and separated on a 1% agarose gel using electrophoresis at 100 V for 45 min, with SYBR® Safe DNA gel stain (Invitrogen) used as a pre-stain. PCR products were then excised from the gel and purified using the GeneJET Gel Extraction Kit (Thermo Fisher Scientific). Briefly, the excised gel portions containing PCR product where solubilized in binding buffer and applied to columns. Columns were centrifuged to capture DNA, and additional centrifugation with wash buffer was performed to remove impurities. DNA was eluted into a sterile microcentrifuge tube and quantified. BP recombination reactions were then performed to clone PCR products into the pDONR™/Zeo entry vector (Invitrogen) following the Gateway® Technology User Guide. Briefly, purified *att*B-PCR products were combined with pDONR™ vector, BP Clonase™ reaction buffer, TE buffer (15.8 g Tris-Cl, 0.5M EDTA, ddH_2O to 250 mL, then diluted 10-fold), and BP Clonase™ enzyme mix before incubating at 25 °C for 1 h. Proteinase K solution was then added, followed by incubation at 37 °C for 10 min. 1-5 µL of this reaction were then added to *Mix & Go!* competent *E. coli* cells (Zymo Research) along with 250 µL S.O.C. medium (Invitrogen), followed by a 1 h incubation with shaking at 37 °C. Cells were then plated on low salt LB + zeocin selection agar plates [3 g tryptone,1.5 g NaCl, 1.5 g yeast extract, ddH_2O to 300 mL, 4.8 g agar, 50 µg/mL zeocin] for identification of successful transformants. Colonies were then

transferred to low salt LB + zeocin media and placed in a 37° C incubator with shaking for 16 h. Entry vector plasmids incorporating the effector candidate genes were isolated from cells using the Monarch® Plasmid Miniprep Kit (New England Biolabs, Inc.). Briefly, cell cultures were centrifuged and the supernatant was removed, followed by resuspension of cell pellets in plasmid resuspension buffer. Plasmid lysis buffer and plasmid neutralization buffer were added to facilitate cell lysis, and the resulting lysate centrifuged to obtain a supernatant. The supernatant was then transferred to a spin column and centrifuged to capture plasmid DNA. This DNA was purified via the addition of wash buffer and additional centrifugation, followed by elution into a sterile microcentrifuge tube using DNA elution buffer. Purified plasmids were then quantified and sequenced to confirm complete and accurate cloning of the candidate genes.

Following confirmation of accurate cloning, LR recombination reactions were performed to transfer candidate genes into the pFPL-Rh destination vector (Gong et al. 2014) following the Gateway® Technology User Guide. Briefly, purified vectors containing candidate genes were combined with the pFPL-Rh destination vector, LR Clonase™ reaction buffer, TE buffer, and LR Clonase™ enzyme mix followed by incubation for 1 h at 25 °C. Proteinase K solution was then added, followed by incubation at 37 °C for 10 min. Competent *E. coli* cells were transformed with this reaction as described above, followed by plating on LB + kanamycin agar [3 g tryptone, 1.5 g yeast extract, 3 g NaCl, ddH_2O to 300 mL, 4.8 g agar, 50 µg/mL kanamycin] and incubation for 24 h at 37 °C. Successful transformants were transferred to LB + kanamycin media and incubated with shaking at 37 °C for 16 h. Plasmids containing candidate genes were purified and isolated using the Monarch® Plasmid Miniprep Kit as described above, followed by quantification. PmeI restriction enzyme was used to linearize plasmids prior to transformation into fungal protoplasts.

2.3.5. Fungal protoplast generation and transformations

Protoplasts were generated using a modified protocol based on the methods described by Liu and Friesen (2012). Briefly, two or more Erlenmeyer flasks containing 60 mL Fries medium [5 g $(NH_4)_2C_4H_4O_6$, 1 g NH_4NO_3, 0.5 g $MgSO_4 \cdot 7H_2O$, 1.3 g KH_2PO_4, 3.41 g $K_2HPO_4 \cdot 3H_2O$, 30 g sucrose, 1 g yeast extract, 2 mL trace element stock solutions (1 L water containing LiCl 167 mg, $CuCl_2 \cdot 2H2O$ 107 mg, H_2MoO_4 34 mg, $MnCl_2 \cdot 4H_2O$ 72 mg, and $CoCl_2 \cdot 4H_2O$ 80 mg) and ddH_2O to 1 L] were inoculated with five dried *P. teres* f. *teres* tissue plugs and incubated with constant rotation at 27 °C for 4 to 7 days. The contents of these flasks were then ground in sterilized blender cups and split between two new 60 mL Fries medium flasks, which were subsequently incubated for 2.5 h under the previously described conditions. Next, the cultures were combined and filtered through Miracloth (EMD Millipore Corp.) before being placed in a petri dish along with 40 mL enzyme-osmoticum [0.6 g lysing enzymes from *Trichoderma harzianum*, 0.1 g β-glucanase from *Trichoderma longibrachiatum*, 40 mL protoplasting buffer extended incubation (58.44 g NaCl, 2.03 g $MgCl*6H_2O$, 9.15 mL 1M KH_2PO_4, 850 uL 1M K_2HPO_4, ddH_2O to 1 L)]. This was then incubated at 30 °C with constant rotation for 4 to 24 h, or until a quantity of 10^7 protoplasts was observed using a hemocytometer. Protoplasts were separated from residual fungal tissue and enzyme-osmoticum via filtration through double-layered Miracloth and centrifuged at 2000 G for 5 min. Supernatant was removed, leaving a damp pellet. If using immediately, ~200 µL of a 4:1 STC:PEG solution was added to the pellet and flicked gently to mix. If the protoplasts were to be used at a later date, 2 µL DMSO was added to the pellet along with the STC:PEG solution, and the resulting mixture stored at -80 °C. Frozen protoplasts were thawed on ice for ~20 min before continuing with the transformation protocol.

Transformation of protoplasts was also performed using a modified version of the methods described by Liu and Friesen (2012). Briefly, ~200 µL of the previously described protoplast:STC:PEG suspension was transferred to a 15 mL tube, with the remainder transferred to additional tubes for use as experimental controls. Depending on the intended transformation, linearized plasmid or sgRNA-Cas9-NLS construct and donor DNA were then added to the transformation tube, gently mixed, and allowed to incubate on ice for 20 min. 200 µL PEG was then added to each tube and mixed, followed by 500 µL and 900 µL PEG in a similar fashion. The tubes were then incubated at room temperature for 20 min. STC was added to each tube as described above but in 1, 3, and 4 mL volumes. Tubes were inverted gently to mix and then centrifuged at 3000 G for 10 min. Supernatant from each tube was then removed down to 400 µL. 800 µL regeneration medium was then added to each tube and gently mixed. An additional 800 µL regeneration medium was added, and any remaining pellet gently triturated. The tubes were then incubated with rocking motion at room temperature for 1.5 to 2.5 h. 20 mL of 35 °C regeneration medium agar was then added to each tube, along with 40 µL of 100 µg/mL hygromycin B to the transformation tube and respective control tube. The tubes were inverted to mix and poured into 100 x 15 mm petri dishes before being placed in a 30 °C incubator.

Fungal colonies visible to the naked eye (3 to 7 days after transformation) were transferred to a potato dextrose agar plate containing hygromycin B and grown in the dark at room temperature for 3 to 5 days. Plates were then placed in the light for 24 h at room temperature followed by the dark for 24 h at 15 °C to induce sporulation. Finally, single spores were isolated and transferred to V8 potato dextrose agar plates [150 mL V8 juice, 10 g Difco PDA, 3 g $CaCO_3$, 10 g agar, and ddH_2O to 1 L] containing 20 µg/mL ampicillin.

2.3.6. PCR and sequence analysis of transformant DNA

PCR analysis was used to verify successful transformants and identify potential off-target or ectopic transformants. For gain-of-function transformants using linearized pFPL-Rh plasmid incorporating a candidate gene, primers designed for amplification of the candidate gene were used to identify if the gene had successfully recombined into the genome. For gene disruption transformants, a primer designed to bind within the hygromycin resistance cassette was used in conjunction with a primer designed to bind outside the target gene to amplify a region of native gene sequence along with a region of hygromycin resistance gene sequence. Additionally, primers designed to bind both upstream and downstream of the target gene were used to amplify the full gene along with the embedded hygromycin resistance cassette.

2.3.7. Bioassays

Inoculations were performed as described by Shjerve et al. (2014). Briefly, fungal isolates were grown on V8 PDA plates for 5 to 7 days at room temperature before being placed in the light at room temperature for 24 h and then placed into the dark at 15 °C for 24 h. Plates were then flooded with 100 mL sterilized distilled water and brushed with an inoculating loop to loosen spores. The resulting solution was then diluted to 2000 spores/mL, and Tween 20 (J.T. Baker Chemical Co.) was added to it at a rate of 1 drop/50 mL to prevent spore clumping. Barley line Beecher was planted in the center of a rack containing 49 cone-tainers (Stuewe & Sons, Inc.) with Tradition barley planted in the outside rows to reduce edge effect. Lines CIho 5791 and Algerian were used as checks for all inoculations. Plants were inoculated at the 2-3 leaf stage (12 to 16 days) by using a paint sprayer (DeVilbiss, model# SRIPRO-635G-10) until leaves were covered homogenously with a fine mist. After inoculation, plants were placed in mist chambers at 100% relative humidity and 21 °C for a 24 h light cycle. Plants were then transferred to a

growth chamber under a 24 h photoperiod at 21 °C, with the phenotype being recorded after 7 days. Disease phenotypes were evaluated based on the 1 to 10 scale developed by Tekauz (1985). Three replicates were completed for each experiment.

2.3.8. Additional marker development

Tissue plugs for all 109 progeny of the FGOH04Ptt-21(FGO21)×BB25 mapping population (hereafter referred to as the "FB" population) were placed into individual Erlenmeyer flasks containing 60 mL of Fries medium and allowed to grow for 5 to 7 days under constant rotation at 27 °C. Tissue was then filtered through Miracloth and washed with sterile distilled water before being dried using a mechanical vacuum and Fisherbrand® P5 filter paper. Dried tissue was then placed into a -20 °C freezer for 10 min before being lyophilized for 24 h or until dried. ~30 mg desiccated tissue was then added to a 2 mL tube containing 300 mg Garnet Matrix A (MP Biomedicals, LLC) and a single 1/4" ceramic bead (MP Biomedicals, LLC). Tubes were shaken at 24 hz using the Retsch® Oscillating Mill MM400 for 2 min. Following the BioSprint DNA Plant Handbook (Qiagen), 500 µL RLT buffer (Qiagen) was added to each tube and tubes were shaken for 2 min as described previously. DNA was then extracted from tissue following the protocols outlined in the BioSprint DNA Plant Handbook. Briefly, the tubes containing fungal tissue and RLT buffer were centrifuged and the supernatant extracted. 5-tube strips (Qiagen) were loaded with isopropanol, MagAttract Suspension G (Qiagen), Buffer RPW (Qiagen), 100% ethanol, nuclease-free water, and the supernatant containing fungal DNA. Loaded 5-tube strips were then placed into the BioSprint 15 (Qiagen), and the "BS15 DNA Plant" protocol was run to extract DNA.

Primer sets were designed as previously described to amplify genomic regions that were polymorphic between FGO21 and BB25. PCR was performed using these primer sets along with

the extracted genomic DNA from all 109 progeny. An additional primer set was used as a positive control when screening for presence/absence polymorphisms. Products were loaded and separated on 1 to 2% agarose gels as previously described for genotype determination. Using MapDisto v2.1.7 (Heffelfinger et al. 2017), the resulting marker data was used to place the new markers on a genetic map alongside the original SNP markers as described by Koladia et al. (2017). Briefly, new markers were added to the previously produced linkage map for the FB population using the "Place locus" command. The "Draw a linkage group" command was used to visualize the incorporation of new markers into the linkage map.

The resulting genotypic data along with the original phenotypic data was analyzed in Qgene v4.4.0 as described in Koladia et al. (2017). Briefly, a critical logarithm of odds (LOD) threshold was calculated by performing 1,000 permutations at a significance level of $\alpha = 0.05$. Composite interval mapping with forward cofactor selection was then performed and the resulting data exported for analysis.

2.4. Results

2.4.1. Candidate identification

A list of effector candidates was created based on gene annotations produced for *P. teres* f. *teres* isolates FGO21 and BB25 (Wyatt et al. 2020). Annotated genes in proximity to the most significant marker underlying the *PttBee1* QTL for both parents were considered as initial candidates, resulting in a combined list of 44 candidate genes (Appendix A). 26 of these candidates were determined to be polymorphic between parents, with an additional candidate supported by expression data for only one parent. Additional selection criteria were used to narrow down this list based on characteristics often associated with fungal effectors. Two candidates were predicted to contain a transmembrane domain by TMHMM v2.0, and no

candidates were predicted to have a GPI cell-surface anchor by NetGPI v1.1. Four candidates were predicted to be secreted by SignalP v5.0, and two of these were predicted to be effectors by EffectorP v.2.0 (Figure 2.1). Additional candidates were identified based on promoter polymorphisms, differences in expression, and non-classical secretion prediction by alternative prediction software.

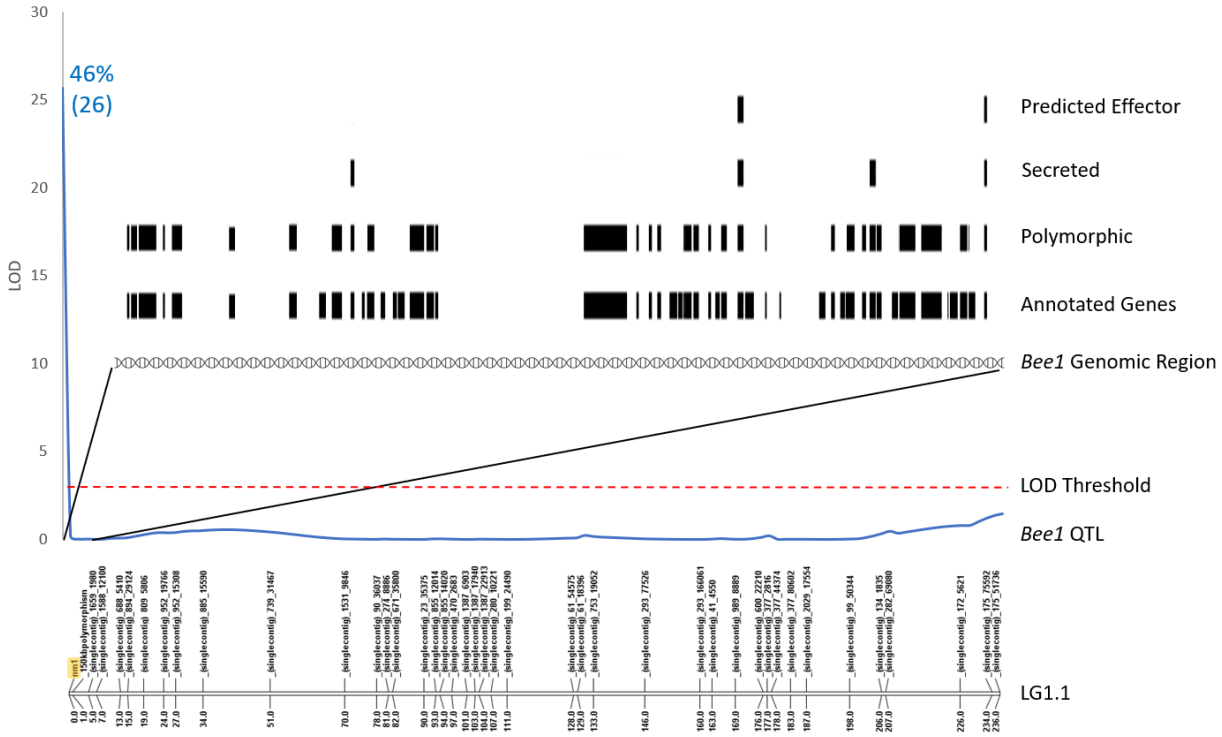

Figure 2.1. Identification of effector candidates. The linkage map of LG1.1 is shown on the bottom, with the most significant marker highlighted in yellow. Above this is the *PttBee1* QTL in blue, and LOD and R^2 values for the peak are in blue. The dashed horizontal line representing the calculated LOD threshold of 3.0. The black blocks represent annotated genes within the *PttBee1* region under increasingly stringent selection criteria. The "Secreted" level indicates polymorphic genes within the *PttBee1* region that were predicted to be secreted by SignalP v5.0. The "Predicted Effector" level indicates secreted proteins that were predicted to be effectors by EffectorP v2.0.

2.4.2. Transformations and bioassays

Eight candidate effectors were used in gain-of-function transformations and/or CRISPR-Cas9 mediated gene disruptions. Gain-of-function transformations were performed by producing

clones of candidate gene alleles from FGO21, the virulent parent, and inserting these genes into the genome of BB25, the avirulent parent. This process involved cloning the genes first into a Gateway® entry vector, and then into a vector optimized for fungal transformations, pFPL-Rh (Gong et al. 2014). This vector contains *Agrobacterium* T-DNA borders to facilitate random recombination into the target genome and a hygromycin resistance cassette for screening of positive transformants. Only two genes were manipulated using this method, as transformation efficiency proved to be much lower than transformations involving CRISPR-Cas9 for gene manipulations.

CRISPR-Cas9 mediated gene disruptions were performed for all eight effector candidates. All genes supported by transcription data were disrupted in the virulent parent, FGO21. The allelic form of four of these candidate effectors were also disrupted in BB25, as the candidate gene may be an effector of avirulence. Candidate *PTT_40000016* was only disrupted in BB25, as there was evidence of expression in this parent but not in FGO21. The QTL analysis performed by Koladia et al. (2017) identified an additional QTL on LG 2.1, *PttBee2*, which accounts for 17% of phenotypic variation. As this region may potentially compensate for a loss in *PttBee1* effector function, gene disruptions were also performed using the FB progeny isolate FB24. This isolate features the FGO21 genotype at the *PttBee1* locus and the BB25 genotype at the *PttBee2* locus, providing additional assurance that successful disruption of a *PttBee1* gene required for virulence would result in a loss of phenotype. Five genes were tested using FB24.

A total of 17 transformants were generated and inoculated on Beecher barley, with no observed change in phenotype from the respective parental isolates or progeny isolate (Table 2.1). Additional transformations must be performed to eliminate the possibility of the *PttBee2*

locus masking a decrease in virulence and/or the possibility of the candidate gene functioning as an effector of avirulence for four of the candidates identified.

Table 2.1. *PttBee1* candidate genes manipulated in this study. The leftmost column lists the candidate genes that were assessed for a potential role in virulence via CRISPR-Cas9 mediated gene disruptions. The rightmost three columns represent the three different fungal isolates in which these genes were manipulated. Red lettering indicates successful gene disruptions. "+" indicates gain-of-function transformations were additionally performed in this isolate.

PttBee1 gene candidates	Virulent parent	FB progeny isolate	Avirulent parent
PTT_40000011	FGO21	FB24	BB25 +
PTT_50000016	FGO21	FB24	BB25
PTT_40000022	FGO21	FB24	BB25
PTT_40000034	FGO21	FB24	BB25 +
PTT_40000036	FGO21	FB24	BB25
PTT_40000042	FGO21	FB24	BB25
PTT_40000043	FGO21	FB24	BB25
PTT_40000052	FGO21	FB24	BB25

2.4.3. Marker development and QTL analysis

Two additional markers were developed to further refine the *PttBee1* QTL and potentially shorten the list of likely effector candidates. The initial analysis performed by Koladia et al. (2017) placed the most significant marker, _(singlecontig)_1659_1980, at position 0.0 on LG1.1, which corresponds to roughly 202 kb from the telomere of FGO21 chromosome 1, and roughly 185 kb from the telomere of BB25 chromosome 1. A 26 bp indel located roughly 149 kb from the chromosome 1 telomere in FGO21 and 127 kb from the chromosome 1 telomere in BB25 was selected to function as the first additional marker. PCR with primers designed to amplify this region was performed using the genomic DNA from 109 progeny in the FB population (Appendix B). This marker data was used alongside the original data to generate an updated genetic map, and QTL analysis identified a greater association with this marker than the original

most significant marker, increasing the LOD value of the *PttBee1* QTL from 19 to 20, and increasing the R^2 value from 43% to 44%. Due to this increased association, an additional primer set was developed to amplify a region roughly 60 kb closer to the telomere in FGO21 and absent in BB25 (Appendix B). QTL analysis using the map produced with this marker resulted in it being identified as the most significant marker, increasing the LOD value to 26 and increasing the R^2 value to 46% (Figure 2.1).

2.5. Discussion

Between 2010 and 2019, barley was the fourth highest produced grain worldwide after maize, wheat, and rice (https://www.fao.org/faostat/en/#compare). In the US, barley is mainly produced for use as animal fodder or in the malting process for alcoholic beverages, but in regions of Africa and Asia it functions as a staple food grain. Barley is susceptible to many different pathogens, with fungi responsible for the majority of barley disease losses worldwide. In Australia, pathogens were estimated to be responsible for an annual loss of barley crop production value equal to roughly 20% of the total yield, and without proper controls losses due to *P. teres* f. *teres* alone could total A$117 million annually (Murray and Brennan 2010).

Multiple methods have been implemented to control fungal pathogens such as *P. teres* f. *teres*, including fungicide application, burying of stubble, and crop rotations, with varying levels of success. Breeding of resistant barley cultivars remains the preferred method for minimizing the threat these pathogens pose to agriculturally significant crops without the negative environmental effects associated with fungicide use. The process of creating lines with durable resistance will benefit from a comprehensive understanding of the interactions between pathogen and host.

The prevailing model used to describe the genetics of host-pathogen interactions was originally put forth as the gene-for-gene model (Flor 1942). This model supposes that for every gene conferring resistance in the host, there is a corresponding gene conferring avirulence in the pathogen. This model has been expanded upon to include pathogen-produced effectors that overcome host resistance to cause disease. In turn, hosts evolve to initiate a defense response upon recognition of these effectors, often resulting in programmed cell death (PCD) and leading again to resistance (Cook et al. 2015; Jones and Dangl 2006). Necrotrophic and hemibiotrophic pathogens often subvert this defense response by inducing PCD and acquiring nutrients from the dying cell tissue, in a model described as inverse gene-for-gene (Friesen and Faris 2010).

In this study, a region of the *P. teres* f. *teres* genome that displayed a high association with virulence was analyzed and 44 genes with potential for conferring this virulence phenotype were identified as effector candidates. In order for one of these genes to be responsible for the observed variation in virulence between isolates, there must be some degree of genomic polymorphism resulting in the expression of non-homologous protein products or variations in expression level. For this reason, candidates were evaluated for coding sequence polymorphisms as well as variation in the predicted promoter regions. As effectors are typically secreted, two proteins containing transmembrane domains or cell surface anchors were eliminated from the candidate list and the remaining genes were analyzed for signal peptides. Two of these secreted candidates were additionally predicted to be effectors. However, there was no decrease or increase in virulence observed after transforming *P. teres* f. *teres* isolates with these genes and inoculating the transformants. For this reason, the selection criteria were expanded to include less obvious candidates. This new candidate list included two proteins that lacked a classical signal peptide but were predicted to be secreted using alternative prediction software, as well as

two candidates with polymorphisms only in the promoter region. Comparative analysis of effector candidates using protein databases indicated that the majority of the tested candidates lacked homology to previously characterized proteins. The predicted amino acid sequences of two candidates, *PTT_40000022* and *PTT_40000034*, displayed homology to an acetylcholinesterase precursor and a cysteine hydrolase, respectively. Eight genes were manipulated in total, but no transformations resulted in a change of virulence.

As any of the remaining candidates could be the potential effector, and transformations in both parents as well as a progeny were needed to rule out any one candidate, new markers were developed to refine the *PttBee1* QTL and help prioritize the candidate list. Two primer sets were developed to genotype the FB population using PCR, resulting in the placement of markers 50 kb and 110 kb away from the original most significant marker in the direction of the telomere. Comparison of genotypic data indicated that recombination occurred between the original marker and the first new marker in three progeny, and recombination occurred between both new markers in a single progeny. Implementation of these markers into the FB genetic map resulted in an increase in the *PttBee1* LOD value from 19 to 26 and an increase in the R^2 value from 43% to 46%, with the new marker closest to the telomere displaying the greatest significance. These increases indicated that the *PttBee1* effector was likely located closer to the telomere, increasing the probability of *PttBee1* being encoded by a more distal candidate. Five genes were annotated in the most distal 20 kb following the telomere, and although none of the genes in this region feature characteristics of classic effectors, they cannot be ruled out without validation (Appendix A). This stepwise delimitation of the *PttBee1* QTL should be repeated up to the telomere itself, if possible, to minimize time spent investigating less probable effector candidates.

Although none of the tested genes were shown to be associated with virulence/avirulence in the interaction of FGO21 and BB25 isolates with Beecher barley, it is possible that these candidates function as effectors against other barley genotypes. Genomes of fungal pathogens are known to contain broad, rapidly evolving effector repertoires, which are especially variable in heterothallic fungi such as *P. teres* and most prevalent in telomeric regions of the genome (Croll and McDonald 2012; Wyatt et al. 2020). Our lab has unpublished data that shows the *PttBee1* region to be associated with virulence on other barley lines, indicating the potential for multiple effectors in this region. It is also possible that instead of a proteinaceous effector underlying the *PttBee1* locus, there may be other explanations for the association including but not limited to a non-proteinaceous small RNA responsible for variations in virulence (Reviewed in Collemare et al. 2019).

In addition to further refinement of the *PttBee1* QTL and manipulation of remaining candidate genes, RNA sequencing at earlier timepoints during the *P. teres* f. *teres* infection cycle could prove to be useful in annotating effector genes only expressed early-on in the infection process. The current annotations are based on transcripts obtained at 48, 72, and 96 hours post-inoculation, however, studies have shown that the pathogen is able to penetrate the plant cell wall and begin acquiring nutrients in as little as 24 hours (Ismail et al. 2014; Keon and Hargraves 1983). Proteomics approaches involving infiltration of tissue lysates or purified proteins could be employed to complement the molecular techniques described here, as these techniques have already shown some success in identifying effectors.

Effector identification will benefit from the gradual increase in data resulting from the identification of novel effectors in all fungal pathogens, possibly shedding light on additional

characteristics shared by this gene class. This data will also be used to further increase the accuracy of prediction software and facilitate informed prioritization of candidate lists.

2.6. Literature cited

Almagro Armenteros, J. J., Sønderby, C. K., Sønderby, S. K., Nielsen, H., and Winther, O. 2017. DeepLoc: Prediction of protein subcellular localization using deep learning. Bioinformatics. 33:3387-3395.

Almagro Armenteros, J. J., Tsirigos, K. D., Sønderby, C. K., Petersen, T. N., Winther, O., Brunak, S., von Heijne, G., and Nielsen, H. 2019. SignalP 5.0 improves signal peptide predictions using deep neural networks. Nat. Biotech. 37:420-423.

Bendtsen, J. D., Jensen, L. J., Blom, N., von Heijne, G., and Brunak, S. 2004. Feature-based prediction of non-classical and leaderless protein secretion. Protein Eng. Des. Sel. 17:349-356.

Clare, S. J., Wyatt, N. A., Brueggeman, R. S., and Friesen, T. L. 2020. Research advances in the *Pyrenophora teres*-barley interaction. Mol. Plant Pathol. 21:272-288.

Collemare, J., O'Connell, R., and Lebrun, M. H. 2019. Nonproteinaceous effectors: The terra incognita of plant-fungal interactions. New Phytol. 223:590-596.

Cook, D. E., Mesarich, C. H., and Thomma, B. P. H. J. 2015. Understanding plant immunity as a surveillance system to detect invasion. Annu. Rev. Phytopathol. 53:541-563.

Croll, D., and McDonald, B. A. 2012. The accessory genome as a cradle for adaptive evolution in pathogens. PloS Pathog. 8:e1002608.

Flor, H. H. 1942. Inheritance of pathogenicity in *Melampsora lini*. Phytopathology. 32:653-669.

Franceschetti, M., Maqbool, A., Jiménez-Dalmaroni, M. J., Pennington, H. G., Kamoun, S., and Banfield, M. J. 2017. Effectors of filamentous plant pathogens: Commonalities amid diversity. Mol. Biol. R. 81:2.

Friesen T. L., and Faris, J. D. 2021. Characterization of effector-target interactions in necrotrophic pathosystems reveals trends and variation in host manipulation. Annu. Rev. Phytopathol. 59:4.1-4.22.

Friesen, T. L., and Faris, J. D. 2010. Characterization of the wheat-*Stagonospora nodorum* system: What is the molecular basis of this quantitative necrotrophic disease interaction? Can. J. Plant Pathol. 32:20-28.

Gíslason, M. H., Nielsen, H., Almagro Armenteros, J. J., and Johansen, A. R. 2021. Prediction of GPI-anchored proteins with pointer neural networks. Curr. Res. Biotech. 3:6-13.

Gong, X., Hurtado, O., Wang, B., Wu, C., Yi, M., Giraldo, M., Valent, B., Goodin, M., and Farman, M. 2015. pFPL Vectors for high-throughput protein localization in fungi: Detecting cytoplasmic accumulation of putative effector proteins. Mol. Plant-Microbe Interact. 28:107-121.

Heffelfinger, C., Fragoso, C. A., and Lorieux, M. 2017. Constructing linkage maps in the genomics era with MapDisto 2.0. Bioinformatics. 33:2224-2225.

Heigwer, F., Kerr, G., and Boutros, M. 2014. E-CRISP: Fast CRISPR target site identification. Nat. Methods. 11:122-123.

Holt, C., and Yandell, M. 2011. MAKER2: An annotation pipeline and genome-database management tool for second-generation genome projects. BMC Bioinformatics. 12:491.

Ismail, I. A., and Able, A. J. 2016. Secretome analysis of virulent *Pyrenophora teres* f. *teres* isolates. Proteomics. 16:2625-2636.

Ismail, I. A., and Able, A. J. 2017. Gene expression profiling of virulence-associated proteins *in planta* during net blotch disease of barley. Physiol. Mol. Plant P. 98:69-79.

Ismail, I. A., Godfrey, D., and Able, A. J. 2014. Fungal growth, proteinaceous toxins and virulence of *Pyrenophora teres* f. *teres* on barley. Australas. Plant Path. 43:535-546.

Jones, D. A., Bertazzoni, S., Turo, C. J., Syme, R. A., and Hane, J. K. 2018. Bioinformatic prediction of plant-pathogenicity effector proteins of fungi. Curr. Opin. Microbiol. 46:43-49.

Jones, J. D. G., and Dangl, J. L. 2006. The plant immune system. Nature. 323-329.

Jones, P., Binns, D., Chang, H. Y., Fraser, M., Li, W., McAnulla, C., McWilliam, H., Maslen, J., Mitchell, A., Nuka, G., Pesseat, S., Quinn, A. F., Sangrador-Vegas, A., Scheremetjew, M., Yong, S. Y., Lopez, R., and Hunter, S. 2014. InterProScan 5: Genome-scale protein function classification. Bioinformatics. 30:1236-1240.

Keon, J. P. R., and Hargreaves, J. A. 1983. A cytological study of the net blotch disease of barley caused by *Pyrenophora teres*. Physiol. Plant Pathol. 22:321-329.

Khan, T. N. and Boyd, W. J. R. 1969. Inheritance of resistance to net blotch in barley. II. Genes conditioning resistance against race W.A.-2. Can. J. Genet. Cytol. 11:592-597.

Koladia, V. M., Richards, J. K., Wyatt, N. A., Faris, J. D., Brueggeman, R. S., and Friesen, T. L. 2017. Genetic analysis of virulence in the *Pyrenophora teres* f. *teres* population BB25×FGOH04Ptt-21. Fungal Genet. Biol. 107:12-19.

Krogh, A., Larsson, B., von Heijne, G., and Sonnhammer, E. L. 2001. Predicting transmembrane protein topology with a hidden Markov model: Application to complete genomes. J. Mol. Biol. 305:567-580.

Liu, Z., and Friesen, T. L. 2012. *Polyethylene glycol (PEG)-mediated transformation in filamentous fungal pathogens*. Methods in molecular biology. Clifton, NJ: 835:365-375.

Liu, Z., Ellwood, S. R., Oliver, R. P., and Friesen, T. L. 2011. *Pyrenophora teres*: Profile of an increasingly damaging barley pathogen. Mol. Plant Pathol. 121:1-19.

Liu, Z., Holmes, D. J., Faris, J. D., Chao, S., Brueggeman, R. S., Edwards, M. C., and Friesen, T. L. 2015. Necrotrophic effector-triggered susceptibility (NETS) underlies the barley–*Pyrenophora teres* f. *teres* interaction specific to chromosome 6H. Mol. Plant Pathol. 16:188–200.

Lo Presti, L., Lanver, D., Schweizer, G., Tanaka, S., Liang, L., Tollot, M., Zuccaro, A., Reissmann, S. and Kahmann, R. 2015. Fungal effectors and plant susceptibility. Annu. Rev. Plant Biol. 66:513-545.

Martin, A., Moolhuijzen, P., Tao, Y., McIlroy, J., Ellwood, S. R., Fowler, R. A., Platz, G. J., Kilian, A., and Snyman, L. 2020. Genomic regions associated with virulence in *Pyrenophora teres* f. *teres* identified by genome-wide association analysis and biparental mapping. Phytopathology. 110:881-891.

Mathre, D. E. 1997. *Compendium of Barley Diseases*, *2nd edn*. St. Paul, MN: American Phytopathological Society.

Murray, G. M., and Brennan, J. P. 2010. Estimating disease losses to the Australian barley industry. Australas. Plant. Path. 39:85-96.

Rapoport, T. A. 2007. Protein translocation across the eukaryotic endoplasmic reticulum and bacterial plasma membranes. Nature. 450:663-669.

Shipton, W. A., Khan, T. N., and Boyd, W. J. R. 1973. Net blotch of barley. Rev. Plant Pathol. 52:269-290.

Shjerve, R. A., Faris, J. D., Brueggeman, R. S., Yan, C., Zhu, Y., Koladia, V., and Friesen, T. L. 2014. Evaluation of a *Pyrenophora teres* f. *teres* mapping population reveals multiple independent interactions with a region of barley chromosome 6H. Fungal Genet. Biol. 70:104-112.

Sperschneider, J., Dodds, P. N., Gardiner, D. M., Singh, K. B., and Taylor, J. M. 2018. Improved prediction of fungal effector proteins from secretomes with EffectorP 2.0. Mol. Plant Pathol. 19:2094-2110.

Tekauz, A. 1985. A numerical scale to classify reactions of barley to *Pyrenophora teres*. Can. J. Plant Pathol. 7:181-183.

Untergasser, A., Cutcutache, I., Koressaar, T., Ye, J., Faircloth, B. C., Remm, M., and Rozen, S. G. 2012. Primer3 - new capabilities and interfaces. Nucleic Acids Res. 40:e115.

Weiland, J. J., Steffenson, B. J., Cartwright, R. D., and Webster, R. K. 1999. Identification of molecular genetic markers in *Pyrenophora teres* f. *teres* associated with low virulence on 'Harbin' barley. Phytopathology. 89:176-181.

Wyatt, N. A., Richards, J. K., Brueggeman, R. S., and Friesen, T. L. 2020. A comparative genomic analysis of the barley pathogen *Pyrenophora teres* f. *teres* identifies subtelomeric regions as drivers of virulence. Mol. Plant-Microbe Interact. 33:173-188.

CHAPTER 3. IDENTIFICATION OF WHEAT QTL ASSOCIATED WITH RESISTANCE/SUSCEPTIBILITY TO *P. TERES* F. *MACULATA*

3.1. Abstract

Emergent pathogens often go undetected until it is too late to prevent an epidemic, and it is therefore imperative that species beginning to exhibit characteristics of emergent pathogens are carefully monitored and safeguarded against. *Pyrenophora teres* f. *maculata* is a foliar pathogen of barley that is present worldwide and growing in prominence in the US and Australia. This pathogen can cause significant yield losses, resulting in efforts to characterize the interaction between *P. teres* f. *maculata* and barley. Of concern, recent reports indicate that this pathogen has made a host jump to wheat, a staple food crop that is responsible for a significant portion of global caloric intake. In this study, a tetraploid wheat panel comprised of local and global *Triticum turgidum* subspecies was screened with four *P. teres* f. *maculata* isolates and a range of resistant to moderately susceptible reaction types was observed. Based on the results of this screening, the progeny of a cross between the moderately susceptible durum line Ben and the resistant cultivated emmer accession PI 41025 were inoculated and the resulting data used for quantitative trait loci (QTL) analysis. To identify associations with resistance/susceptibility in the broader durum wheat population, the *P. teres* f. *maculata* isolate FGOB10Ptm-1 was inoculated on a representative subset of the Global Durum Wheat Panel (GDP), and a genome-wide association study performed using the resulting data. Results of both mapping studies indicate a major association with resistance/susceptibility to *P. teres* f. *maculata* on the short arm of durum wheat chromosome 2A. Additionally, a minor association on the long arm of chromosome 4B was identified from the GWAS data.

3.2. Introduction

Emergent pathogens can be classified as any pathogen that has become the causal agent of a new disease or displayed increased incidence of disease, expanded its geographic range, shown alterations in pathogenicity, or caused disease on a novel host (Anderson et al. 2004; Corredor-Moreno and Saunders 2020). Emergent pathogens of food crops have the potential to cause widespread crop destruction, resulting in significant agricultural and economic loss as well as loss of human life (Reviewed in Fones et al. 2020). Examples include the introduction of *Phytophthora infestans* to Europe, resulting in the Irish potato famine of the 1840s (Yoshida et al. 2013); the Bengal famine of 1943, caused by massive shortages of rice attributed to an outbreak of *Cochliobolus miyabeanus* (Padmanabhan 1973); the United States southern corn leaf blight epidemic of 1970, caused by *Cochliobolus heterostrophus* race T (Ullstrup 1972), and the modern-day spread of Fusarium wilt caused by *Fusarium oxysporum* f. sp. *cubense* tropical race 4, threatening the global production of Cavendish bananas (Vézina 2021). One of the most recent instances of a major pathogen emergence is that of the devastating rice pathogen *Magnaporthe oryzae* as a pathogen of wheat (Reviewed in Cruz and Valent 2017). First observed in Brazil in 1985 (Igarashi et al. 1986), the *Triticum* pathotype of *M. oryzae* (*MoT*) has spread throughout South America (Valent et al. 2021) and more recently to South Asia (Malaker et al. 2016) and Africa (Tembo et al. 2020). Wheat blast epidemics can result in up to 100% yield loss, emphasizing the significance of host jumps resulting in pathogen emergence (Valent et al. 2021). Factors contributing to increased pathogen emergence include the introduction of invasive species, planting of crop monocultures, agricultural globalization and intensification, and climate change (Reviewed in Anderson et al. 2004). As emergent plant pathogens will continue to pose a

major threat to modern agricultural systems and staple food crops, it is imperative that these pathogens are identified, monitored, and safeguarded against.

Pyrenophora teres f. *maculata* is a filamentous fungal pathogen causing spot form net blotch (SFNB) of barley. SFNB is characterized by round or oval shaped necrotic foliar lesions with a chlorotic halo that may coalesce and result in death of the leaf under favorable conditions (Shipton et al. 1973; Smedegård-Petersen 1971). Though present in barley growing regions worldwide, *P. teres* f. *maculata* has recently increased in prominence in the United States and Australia, causing yield losses of up to 44% (Liu et al. 2010; Marshall et al. 2015; McClean et al. 2010; Jayasena et al. 2007). Additionally, first reports of the pathogen causing disease on wheat have come out of Hungary (Tóth et al. 2008) and Russia (Mikhailova et al. 2010).

The most recent reports of *P. teres* f. *maculata* infecting wheat leaves have emerged from Argentina, where lesions similar in morphology to those of SFNB were identified during routine field surveys (Perelló et al. 2019). Following Koch's postulates, spores of the pathogen were isolated and re-infected on wheat under greenhouse conditions. Sequencing of the internal transcribed spacer as well as PCR with form-specific primers confirmed the infecting fungus to be *P. teres* f. *maculata*, validating its status as a pathogen of wheat (Perelló et al. 2019). Following this study, two of the Argentinian isolates were inoculated on a diverse set of previously genotyped spring wheat lines, resulting in the identification of 12 marker-trait associations involving nine markers, three of which had not previously been associated with disease resistance/susceptibility (Uranga et al. 2020).

In this study, a tetraploid wheat diversity panel was screened with *P. teres* f. *maculata* reference isolates to identify resistant and susceptible durum wheat lines. Resistance/susceptibility to *P. teres* f. *maculata* was further investigated using the wheat

biparental mapping population BP025, consisting of the recombinant inbred progeny of a cross between durum wheat line Ben and the cultivated emmer wheat accession PI 41025 (Faris et al. 2014). The resulting phenotypic data was used to map quantitative trait loci (QTL) associated with resistance/susceptibility to a diverse set of *P. teres* f. *maculata* isolates. Finally, *P. teres* f. *maculata* isolate FGOB10Ptm-1 (Syme et al. 2018) was inoculated on a portion of the Global Durum Wheat Panel (GDP) (Mazzucotelli et al. 2020) and a genome wide association study (GWAS) was performed to further identify markers and the genomic location associated with resistance/susceptibility.

3.3. Materials and methods

3.3.1. Biological materials

P. teres f. *maculata* isolates used in this study included C-A17 and P-A14 collected from Celebration barley and Pinnacle barley, respectively, in Montana, USA in 2012 (Wyatt and Friesen 2021); FGOB10Ptm-1 collected from barley in North Dakota, USA in 2010 (Carlsen et al. 2017; Syme et al. 2018), and Den2.6 collected from barley in Denmark (Wyatt and Friesen 2021). These laboratory reference isolates were chosen based on their inclusion in prior mapping studies and currently available genomic resources (Carlsen et al. 2017; Syme et al. 2018; Wyatt and Friesen 2021).

A set of 90 globally diverse tetraploid wheat lines were selected as a diversity panel for screening of *P. teres* f. *maculata* isolates. The BP025 wheat biparental recombinant inbred population was developed from durum wheat line Ben, a North Dakota hard amber durum variety, and cultivated emmer accession PI 41025, collected near Samara, Russia (Faris et al. 2014). A representative set of 510 durum wheat accessions were selected from the Global Durum Wheat Panel, as testing of all 1,011 lines was not feasible (Mazzucotelli et al. 2020).

3.3.2. Phenotyping

Inoculations were performed as described by Shjerve et al. (2014). Briefly, fungal isolates were grown on V8 potato dextrose agar (V8 PDA) medium plates (150 mL V8 juice, 10 g Difco PDA, 3 g $CaCO_3$, 10 g agar, and ddH_2O to 1 L) for 5 to 7 days at room temperature before being placed in the light at room temperature for 24 h and then placed into the dark at 15 °C for 24 h to induce sporulation. Plates were then flooded with 100 mL sterilized distilled water and brushed with an inoculating loop to loosen spores. The resulting solution was then diluted to 2000 spores/mL, and Tween 20 (J.T. Baker Chemical Co.) was added at a rate of 1 drop/50 mL to prevent spore clumping. Wheat lines for all experiments were planted in racks containing 96 cone-tainers (Stuewe & Sons, Inc.), with Tradition barley or Alsen wheat planted in the outside rows to reduce edge effect. Seedlings were inoculated using a paint sprayer (DeVilbiss, model# SRIPRO-635G-10) when secondary leaves had become fully expanded (14 to 16 days). Leaves were covered homogenously with a heavy mist of inoculum but prior to runoff. After inoculation, plants were placed in mist chambers at 100% relative humidity and 21 °C for a 24 h light cycle. Plants were then transferred to a growth chamber under a 24 h photoperiod at 21 °C. Disease reactions were evaluated after 7 days on a 1 to 5 scale as in Neupane et al. (2015), where a 1-type reaction represented a high level of resistance, and a 5-type reaction represented high susceptibility. The BP025 population, tetraploid panel, and GDP representative set were phenotyped for 3 replications for each isolate used.

3.3.3. QTL analysis

A total of 2,593 markers were used in the formation of the 14 linkage groups that corresponded to the 14 chromosomes present in tetraploid wheat (Faris et al. 2014). Levene's test (Levene 1960) was used to determine homogeneity of variance between replications, and the

average disease score for each isolate was converted into a weighted rank used as phenotypic data for QTL analysis. QTL analysis was conducted in QGene 4.4.0 (Joehanes and Nelson 2008) using composite interval mapping with forward cofactor selection. Permutation tests using 1,000 iterations were performed to establish initial critical logarithm of odds (LOD) thresholds at a significance level of $\alpha = 0.05$ for each isolate inoculated on the BP025 population. A critical LOD threshold of 3.4 was selected as the cutoff for significance for any one QTL, based on the highest overall threshold value observed.

3.3.4. GWAS

Data obtained from three replications of inoculations of the GDP subset with isolate FGOB10Ptm-1 were pooled and Levene's test was used to determine homogeneity of variance at a $P = 0.001$ level of significance. A hapmap containing data for 13,173 SNP markers (Mazzucotelli et al. 2020) was filtered for a minimum allele frequency of 0.05 and a minimum count of 459, resulting in 12,223 markers. Kinship was calculated and a principal component analysis performed to control for population structure using built-in tools in TASSEL v5.2.75 (Bradbury et al. 2007). A GWAS was performed using the mixed linear model in TASSEL and the significance threshold was calculated using the Benjamini-Hochberg false discovery rate (Benjamini and Hochberg 1995). A Manhattan plot was generated using the qqman package in R (Turner 2018).

3.4. Results

3.4.1. Phenotyping

To identify susceptible wheat lines, a tetraploid wheat diversity panel containing 90 globally diverse wheat lines was screened with *P. teres* f. *maculata* isolates C-A17, Den2.6, FGOB10Ptm-1, and P-A14 (Appendix D). A range of average disease scores from 1.0 to 3.17

was observed, indicating that *P. teres* f. *maculata* isolates can cause disease on select tetraploid wheat lines. The durum wheat line Ben was found to be moderately susceptible to all isolates, necessitating further investigation using the BP025 population for characterization of this susceptibility. Inoculations of 117 progeny of the BP025 population showed a range of disease reactions to the four *P. teres* f. *maculata* isolates, with isolate P-A14 exhibiting the highest average disease reaction across the BP025 progeny lines (Figure 3.1, Appendix D). An average disease reaction of 1.0 was recorded for all isolates on PI 41025, and average disease reactions of 2.0 to 2.8 were recorded for Ben (Figure 3.2, Table 3.1). Inoculations of the GDP representative set produced a range of average disease reactions from 1.0 to 4.83 (Figure 3.3, Appendix E).

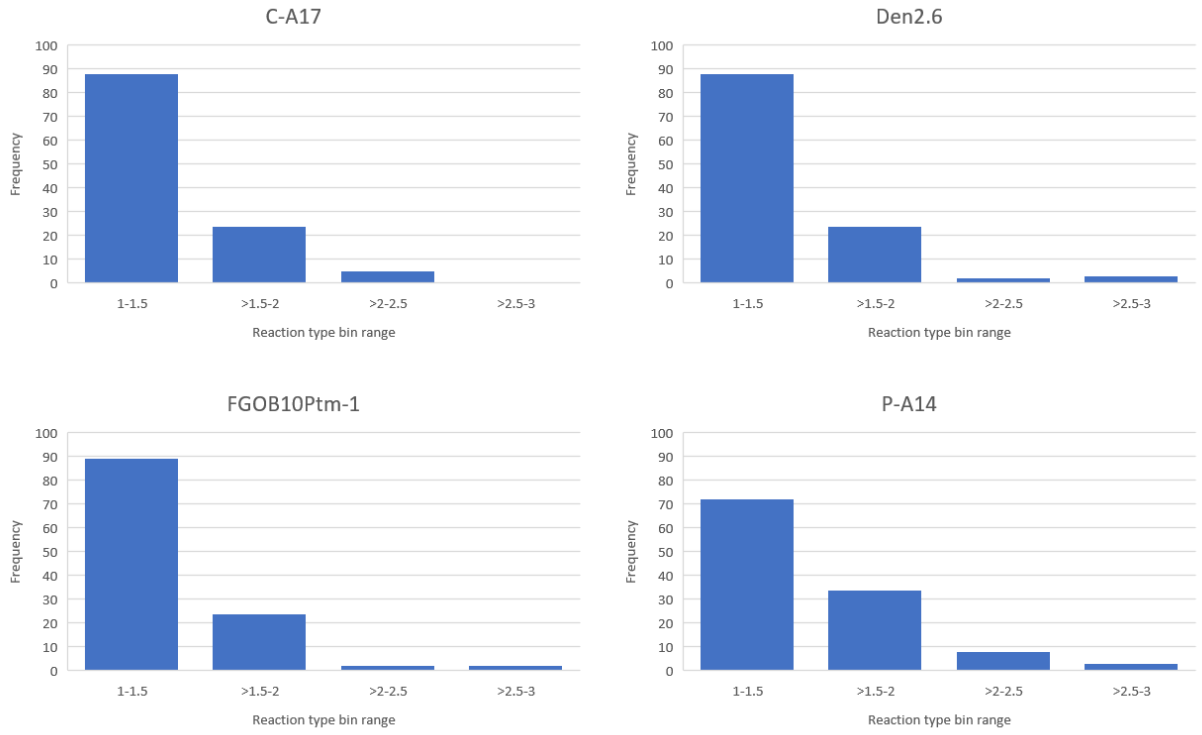

Figure 3.1. Histograms representing average disease reactions of progeny isolates of the BP025 population when inoculated with *P. teres* f. *maculata* isolates C-A17, Den2.6, FGOB10Ptm-1, and P-A14. The *x*-axis represents average disease reaction scores of the BP025 progeny, and the *y*-axis represents the frequency of progeny exhibiting these scores.

Table 3.1. Average disease reaction types of parental lines.

Isolate	Ben	PI 41025
C-A17	2.7	1
Den2.6	2.3	1
FGOB10Ptm-1	2.0	1
P-A14	2.8	1

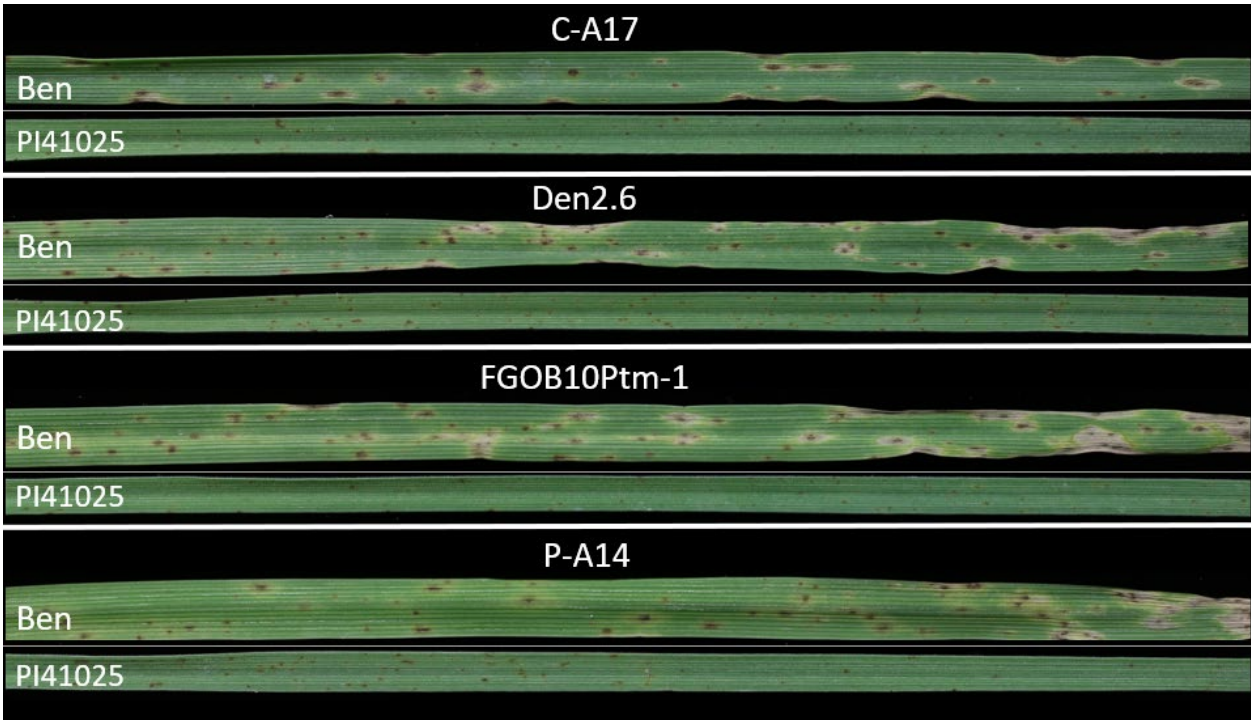

Figure 3.2. Disease reactions on parental wheat lines Ben and PI 41025 inoculated with *P. teres* f. *maculata* isolates C-A17, Den2.6, FGOB10Ptm-1, and P-A14.

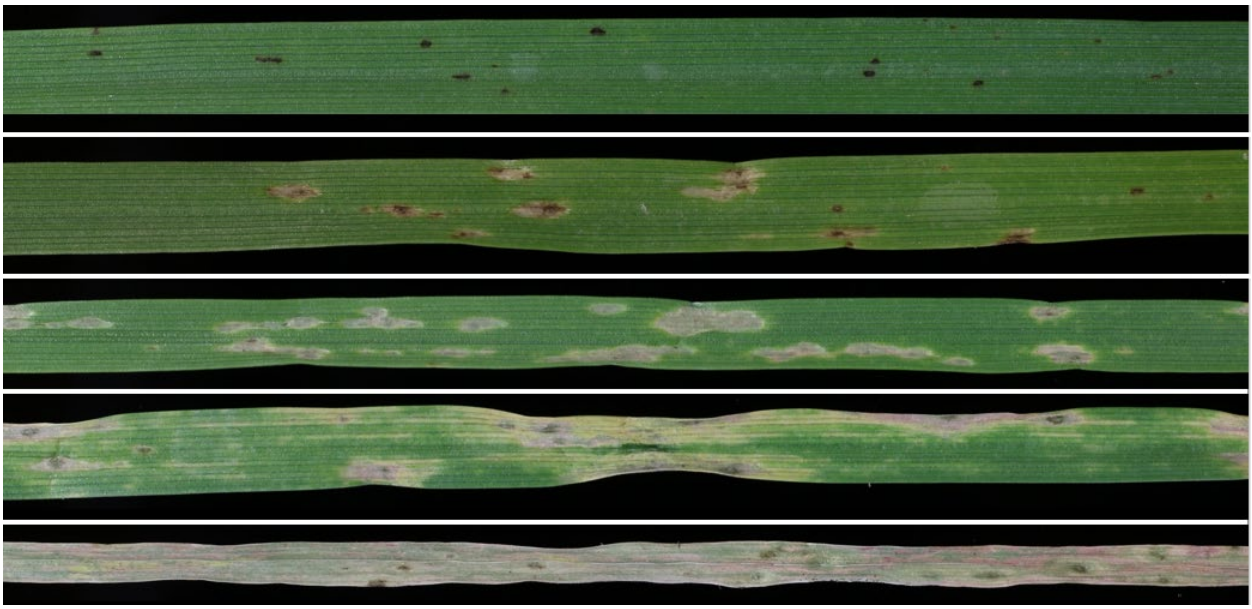

Figure 3.3. Range of phenotypes observed on a representative set of the Global Durum Wheat Panel inoculated with isolate FGOB10Ptm-1. Leaves are arranged top to bottom in order of increasing susceptibility.

3.4.2. QTL analysis

To identify regions within the durum wheat genome associated with resistance/susceptibility to *P. teres* f. *maculata* isolates, QTL analyses were performed using the previously collected phenotypic data and the BP025 genetic map. A QTL was deemed significant if it surpassed a critical LOD threshold of 3.4, which was the highest overall value identified using 1,000 permutations and an $\alpha = 0.05$ level of significance (Appendix F). For the four *P. teres* f. *maculata* isolates tested on the BP025 population, only one significant QTL was identified, corresponding to durum wheat chromosome 2A (Figure 3.4). This QTL accounted for 25% of the phenotypic variation for isolate FGOB10Ptm-1 (LOD = 7.4), 19% for C-A17 (LOD = 5.4), 15% for P-A14 (LOD = 4.0), and 13% for Den2.6 (LOD = 3.4).

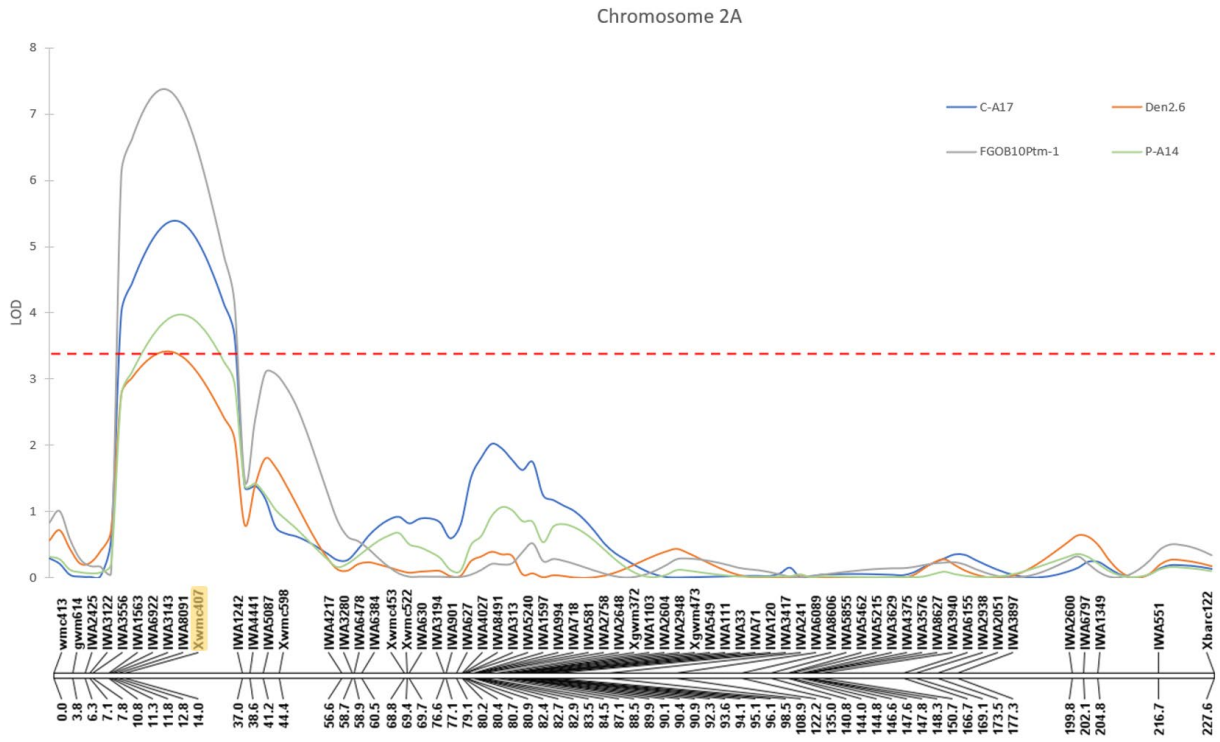

Figure 3.4. QTL associated with disease resistance/susceptibility to each of the four *P. teres* f. *maculata* isolates tested on the BP025 population. The genetic map of durum wheat chromosome 2A with markers and genetic distances is shown underneath the composite interval mapping curve, with the most significant marker highlighted. LOD scales (0 to 8) are shown on the *y*-axis. The dashed red line represents the LOD significance threshold of 3.4.

3.4.3. GWAS

GWAS analysis was performed to identify regions associated with resistance/susceptibility using a subset of the GDP. The *P. teres* f. *maculata* isolate FGOB10Ptm-1 was used to phenotype this population based on the high level of virulence observed during screening of the tetraploid wheat diversity panel. A false discovery rate significance threshold of 4.4 was used to identify significantly associated markers. Ten significant associations were identified, nine of which corresponded to chromosome 2A and one corresponding to chromosome 4B (Figure 3.5). The most significant marker on chromosome 2A had a $-\log_{10}(p)$ value of 19.4 and contributed 18% of the phenotypic variation. The significant

marker on chromosome 4B had a -$\log_{10}(p)$ value of 4.6 and was responsible for 4% of the phenotypic variation.

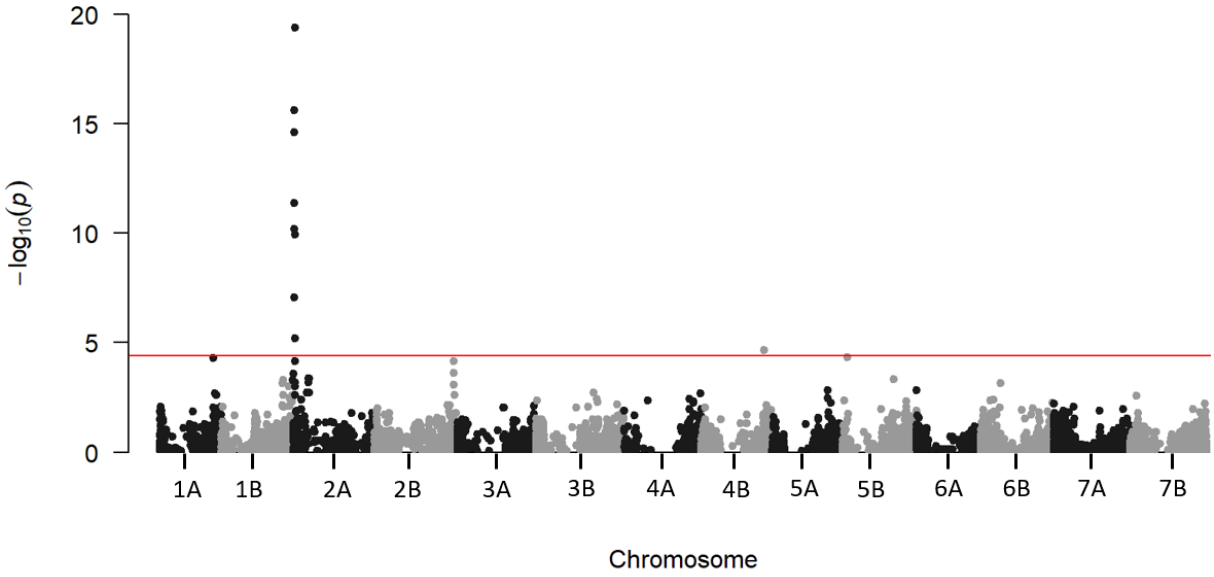

Figure 3.5. Manhattan plot of the genome-wide analysis to identify durum wheat genomic markers associated with resistance/susceptibility to *P. teres* f. *maculata* isolate FGOB10Ptm-1. Durum wheat chromosomes are indicated on the *x*-axis, and marker association with resistance/susceptibility indicated on the *y*-axis. The red line represents the significance threshold of 4.4.

3.5. Discussion

The UN-FAO predicts that food production must increase by 50% by 2050 to meet the demands of a rapidly growing global population (FAO 2017). Responsible for roughly 20% of caloric intake worldwide, wheat production will need to increase to help meet this demand. Efforts to increase wheat production are currently hampered by a wide variety of fungal diseases, including tan spot, Fusarium head blight, septoria tritici blotch, spot blotch, septoria nodorum blotch, and leaf, stripe, and stem rust, which account for global annual crop losses to diseases estimated at 17% (Savary et al. 2019). In addition to these classical diseases of wheat, wheat blast caused by the recently diverged *Magnaporthe oryzae* pathotype, *MoT*, has taken hold in regions of South America, Asia, and Africa. This pathogen has caused multiple epidemic-level

events after being first identified in 1985, with major yield losses recorded in Brazil (Goulart and Paiva 1992), Bolivia (Barea and Toledo 1996), Paraguay (Viedma and Morel 2002), and Bangladesh (Islam et al. 2016). Similar to *MoT*, *P. teres* f. *maculata* has been identified as a recent emergent pathogen of both bread and durum wheat and should be taken seriously by breeders to avoid future epidemics.

Durum wheat represents 5 to 8% of the total global wheat production and is the fifth most produced class of wheat in the US. This species is adapted to a wider range of environments than bread wheat, and in the US is grown primarily in North Dakota and Montana, as the crop does well under the warm, dry conditions typical of this region. To characterize potential susceptibility of durum wheat to *P. teres* f. *maculata*, 90 globally diverse tetraploid wheat lines were screened, including common North Dakotan varieties. Of these, the highest level of susceptibility was observed for the variety Ben inoculated with North Dakotan *P. teres* f. *maculata* isolate FGOB10Ptm-1. The prevalence of *P. teres* f. *maculata* in this region has increased significantly in recent years, though as of yet it has only been reported on its classical host, barley. However, based on the moderate level of susceptibility recorded for Ben as well as other local wheat varieties such as Divide and Dilse, it is possible that this pathogen has adapted to cause disease on these local varieties and has so far gone undetected. The phenotypic similarities between disease caused by this pathogen and tan spot caused by *Pyrenophora tritici-repentis*, also prevalent in the North Dakota-Montana growing region, make this scenario especially plausible.

Based on the results of the initial screening, the Ben × PI 41025 population was selected as the population for mapping of QTL associated with resistance/susceptibility. Data gathered for four *P. teres* f. *maculata* isolates produced the same association on the short arm of durum

chromosome 2A, with local isolate FGOB10Ptm-1 producing the largest QTL in terms of LOD value and association with variation in phenotype. Subsequently, this isolate was chosen for GWAS analysis using a representative subset of the GDP. A major association was identified corresponding to the same region of chromosome 2A, indicating that the loci conferring resistance/susceptibility in local wheat varieties is likely conserved in the global population.

Alignment of the most significant markers observed in both QTL and GWAS analysis to the durum wheat reference genome, Svevo, placed these associations at a physical distance of 7.5 Mbp and 16.5 Mbp from the short arm telomere of chromosome 2A, respectively. The Svevo genome was estimated to be 10.45 Gbp (Maccaferri et al. 2019) in size, and marker densities were calculated to be one marker per 0.94 cM and one SNP per 1.7 Mbp for the BP025 population and GDP, respectively. Based on these data, it is likely that the associations observed for both experiments correspond to the same resistance or susceptibility gene. Interestingly, this region of 2A has previously been characterized as associating with resistance/susceptibility of durum wheat to Fusarium head blight, indicating that the region may potentially be commonly involved in disease resistance (Garvin et al. 2009; Ghavami et al. 2011). Additionally, GWAS analysis by Uranga et al. (2020) identified associations with resistance on two regions of spring wheat chromosome 2D, though it is not known if these regions are homoelogous to the 2A locus identified here.

Taken together, the results of this study indicate that resistance/susceptibility in wheat to the emergent pathogen *P. teres* f. *maculata* is present on both a local and global scale. The same can be said regarding pathogenicity of *P. teres* f. *maculata*, as both the Danish isolate and North American isolates displayed moderate levels of virulence on several durum wheats. Given the moderate level of susceptibility observed in popular local cultivars, efforts should be made to

identify all occurrences of this pathogen on wheat, as well as to identify potential sources of resistance or elimination of susceptibility that could be incorporated into local breeding programs. Natural and biparental *P. teres* f. *maculata* populations are being used to identify pathogen loci associated with virulence and to create a more representative picture of the interaction between this emergent pathogen and durum wheat. Significant efforts should be taken to prevent *P. teres* f. *maculata* from becoming a devastating pathogen of bread and durum wheat.

3.6. Literature cited

Anderson, P. K., Cunningham, A. A., Patel, N. G., Morales, F.J., Epstein, P. R., and Daszak, P. 2004. Emerging infectious diseases of plants: Pathogen pollution, climate change and agrotechnology drivers. Trends Ecol. Evol. 19:535-544.

Barea, G., and Toledo, J. 1996. *Identificación y Zonificación de Pyricularia o brusone (Pyricularia oryzae) en el cutivo de trigo en el Departamento de Santa Cruz*. Informe Tecnico. Proyecto de Investigacion Trigo. Santa Cruz de la Sierra: Centro de Investigación Agrícola Tropical. 76-86.

Benjamini, Y., and Hochberg, Y. 1995. Controlling the false discovery rate: A practical and powerful approach to multiple testing. J. Roy. Stat. Soc. B. 57:289-300.

Bradbury, P. J., Zhang, Z., Kroon, D. E., Casstevens, T. M., Ramdoss, Y., and Buckler, E. S. 2007. TASSEL: Software for association mapping of complex traits in diverse samples. Bioinformatics. 23:2633-2635.

Carlsen, S. A., Neupane, A., Wyatt, N. A., Richards, J. K., Faris, J. D., Xu, S. S., Brueggeman, R. S., and Friesen, T. L. 2015. Characterizing the *Pyrenophora teres* f. *maculata*-barley interaction using pathogen genetics. G3-Genes Genom. Genet. 7:2615-262.

Corredor-Moreno, P., and Saunders, D. G. O. 2020. Expecting the unexpected: Factors influencing the emergence of fungal and oomycete plant pathogens. New Phytol. 225:118-125.

Cruz, C. D., and Valent, B. 2017. Wheat blast disease: Danger on the move. Trop. Plant Pathol. 42:210-222.

FAO. 2017. The future of food and agriculture–trends and challenges. Rome: FAO. Available at: http://www.fao.org/publications/fofa. (Accessed January 30, 2021).

Faris, J. D., Zhang, Q., Chao, S., Zhang, Z. and Xu, S. S. 2014. Analysis of agronomic and domestication traits in a durum × cultivated emmer wheat population using a high-density single nucleotide polymorphism-based linkage map. Theor. Appl. Genet. 127:2333-2348.

Fones, H. N., Bebber, D. P., Chaloner, T. M., Kay, W. T., Steinberg, G., and Gurr, S. J. 2020. Threats to global food security from emerging fungal and oomycete crop pathogens. Nat. Food. 1:332-342.

Garvin, D. F., Stack, R. W., and Hansen, J. M. 2009. Quantitative trait locus mapping of increased Fusarium head blight susceptibility associated with a wild emmer wheat chromosome. Phytopathology. 99:447-452.

Ghavami, F., Elias, E. M., Mamidi, S., Ansari, O., Sargolzaei, M., Adhikari, T., Mergoum, M., and Kianian, S. F. 2011. Mixed model association mapping for Fusarium head blight resistance in Tunisian-derived durum wheat populations. G3-Genes Genom. Genet. 1:209-218.

Goulart, A. C. P., and Paiva, F. A. 1992. Incidence of (*Pyricularia oryzae*) in different wheat cultivars under field conditions. Fitopatol. Bras. 17:321-325.

Igarashi, S., Utiamada, C. M., Igarashi, L. C., Kazuma, A. H., and Lopes, R., S. 1986. Pyricularia em trigo. 1. Ocorrência de *Pyricularia* sp. no estado do Paraná. Fitopatol. Bras. 11:351-352.

Islam, M. T., Croll, D., Gladieux, P., Soanes, D. M., Persoons, A., Bhattacharjee, P., Hossain, M. S., Gupta, D. R., Rahman, M. M., Mahboob, M. G. and Cook, N. 2016. Emergence of wheat blast in Bangladesh was caused by a South American lineage of *Magnaporthe oryzae*. BMC Biol. 14:1-11.

Jayasena, K. W., Van Burgel, A., Tanaka, K., Majewski, J., and Loughman, R. 2007. Yield reduction in barley in relation to spot-type net blotch. Australas. Plant. Path. 36:429-433.

Joehanes, R., and Nelson, J. C. 2008. QGene 4.0, an extensible Java QTL-analysis platform. Bioinformatics. 24:2788-2789.

Levene, H. 1960. *In Contributions to Probability and Statistics: Essays in Honor of Harold Hotelling, I.* Olkin et al. eds., Stanford University Press. 278-292.

Liu, Z. H., and Friesen, T. L. 2010. Identification of *Pyrenophora teres* f. *maculata*, causal agent of spot type net blotch of barley in North Dakota. Plant Dis. 94:480.

Maccaferri, M., Harris, N. S., Twardziok, S. O., Pasam, R. K., Gundlach, H., Spannagl, M., Ormanbekova, D., Lux, T., Prade, V. M., Milner, S. G., Himmelback, A., Mascher, M., Bagnaresi, P., Faccioli, P., Cozzi, P., Lauria, M., Lazzari, B., Stella, A., Manconi, A., Gnocchi, M., Coscatelli, M., Avni, R., Deek, J., Biyiklioglu, S., Frascaroli, E., Corneti, S., Salvi, S., Sonnante, G., Desiderio, F., Mare, C., Crosatti, C., Mica, E., Ozkan, H., Kilian, B., De Vita, P., Marone, D., Joukhadar, R., Mazzucotelli, E., Nigro, D., Gadaleta, A., Chao, S., Faris, J. D., Melo, A. T. O., Pumphrey, M., Pecchioni, N., Milanesi, L., Wiebe, K., Ens, J., MacLachlan, R. P., Clarke, J. M., Sharpe, A. G., Koh, C. S., Liang, K. Y. H., Taylor, G. J., Knox, R., Budak, H., Mastrangelo, A. M., Xu, S. S., Stein, N., Hale, I., Distelfeld, A., Hayden, M. J., Tuberosa, R., Walkowiak, S., Mayer, K. F. X, Ceriotti,

A., Pozniak, C. J., and Cattivelli, L. 2019. Durum wheat genome highlights past domestication signatures and future improvement targets. Nat. Genet. 51:885-895.

Malaker, P. K., Barma, N. C. D., Tiwari, T. P., Collis, W. J., Duveiller, E., Singh, P. K., Joshi, A. K., Singh, R. P., Braun, H. J., Peterson, G. L., Pedley, K. F., Farman, M. L., and Valent, B. 2016. First report of wheat blast caused by *Magnaporthe oryzae* pathotype *triticum* in Bangladesh. Plant Dis. 100:2330-2330.

Marshall, J. M., Kinzer, K., and Brueggeman, R. S. 2015. First report of *Pyrenophora teres* f. *maculata* the cause of spot form net blotch of barley in Idaho. Plant Dis. 99:1860.

Mazzucotelli, E., Sciara, G., Mastrangelo, A. M., Desiderio, F., Xu, S. S., Faris, J., Hayden, M. J., Tricker, P. J., Ozkan, H., Echenique, V., Steffenson, B. J., Knox, R., Niane, A. A., Udupa, S. M., Longin, F. C. H., Marone, D., Petruzzino, G., Corneti, S., Ormanbekova, D., Pozniak, C., Roncallo, P. F., Mather, D., Able, J. A., Amri, A., Braun, H., Ammar, K., Baum, M., Cattivelli, L., Maccaferri, M., Tuberosa, R., and Bassi, F. M. 2020. The Global Durum Wheat Panel (GDP): An international platform to identify and exchange beneficial alleles. Front. Plant. Sci. 11:569905.

McLean, M. S., Howlett, B. J., and Hollaway, G. J. 2010. Spot form of net blotch, caused by *Pyrenophora teres* f. *maculata,* is the most prevalent foliar disease in Victoria, Australia. Australas. Plant Path. 39:46-49.

Mikhailova, L. A., Ternyuk, I. G., and Mironenko, N. V. 2010. *Pyrenophora teres*, an agent causing wheat leaf spot. Microbiology. 79:561-565.

Neupane, A., Tamang, P., Brueggeman, R. S., and Friesen, T. L. 2015. Evaluation of a barley core collection for spot form net blotch reaction reveals distinct genotype-specific pathogen virulence and host susceptibility. Phytopathology. 105:509-517.

Padmanabhan, S. Y. 1973. The great Bengal famine. Annu. Rev. Phytopathol. 11:11-24.

Perelló, A. E., Couretot, L., Curti, A., Uranga, J. P. and Consolo, V. F. 2019. First report of spot lesion of wheat caused by *Pyrenophora teres* f. sp *maculata* observed in Argentina. Crop. Prot. 122:19-22.

Savary, S., Willocquet, L., Pethybridge, S. J., Esker, P., McRoberts, N., and Nelson, A. 2019. The global burden of pathogens and pests on major food crops. Nat. Ecol. Evol. 3:430-439.

Shipton, W. A., Khan, T. N., and Boyd, W. J. R. 1973. Net blotch of barley. Rev. Plant Pathol. 52:269-290.

Shjerve, R. A., Faris, J. D., Brueggeman, R. S., Yan, C., Zhu, Y., Koladia, V., and Friesen, T. L. 2014. Evaluation of a *Pyrenophora teres* f. *teres* mapping population reveals multiple independent interactions with a region of barley chromosome 6H. Fungal Genet. Biol. 70:104-112.

Smedegård-Petersen, V. 1971. *Pyrenophora teres f. maculata f. nov. and Pyrenophora teres f. teres on barley in Denmark.* Copenhagen: Yearbook of the Royal Veterinary and Agricultural University. 124-144.

Syme, R. A., Martin, A., Wyatt, N. A., Lawrence, J. A., Muria-Gonzalez, M. J., Friesen, T. L., Ellwood, S. R. 2018. Transposable element genomic fissuring in *Pyrenophora teres* is associated with genome expansion and dynamics of host-pathogen genetic interactions. Front. Gen. 9:130.

Tembo, B., Mulenga, R. M., Sichilima, S., M'siska, K. K., Mwale, M., Chikoti, P. C., Singh, P. K., He, X., Pedley, K. F., Peterson, G. L., Singh, R. P., and Braun, H. J. 2020. Detection and characterization of fungus (*Magnaporthe oryzae pathotype Triticum*) causing wheat blast disease on rain-fed grown wheat (*Triticum aestivum* L.) in Zambia. PloS One 15:e0238724.

Tóth, B., Csősz, M., Kopahnke, D. and Varga, J. 2008. First report on *Pyrenophora teres* causing lesions of wheat leaves in Hungary. Plant Pathol. 57.

Turner 2018. qqman: An R package for visualizing GWAS results using Q-Q and manhattan plots. J. Open Source Softw. 3:731.

Ullstrup, A. J. 1972. The impacts of the southern corn leaf blight epidemics of 1970-1971. Annu. Rev. Phytopathol. 10:37-50.

Uranga, J. P., Schierenbeck, M., Perelló, A. E., Lohwasser, U., Börner, A., and Simón, M. R. 2020. Localization of QTL for resistance to *Pyrenophora teres f. maculata*, a new wheat pathogen. Euphytica. 216:56.

Valent, B., Cruppe, G., Stack, J. P., Cruz, C. D., Farman, M. L., Paul, P. A., Peterson, G. L, and Pedley, K. F. 2021. Recovery plan for wheat blast caused by *Magnaporthe oryzae pathotype Triticum.* Plant Health Prog. 22:182-212.

Vézina, A. 2021. Tropical Race 4. Musapedia, the banana knowledge compendium. Available at: https://www.promusa.org/Tropical+race+4+-+TR4. (Accessed October 14, 2021).

Viedma, L. Q., and Morel, W. 2002. A~nublo o Piricularia del Trigo (WheatBlast). D'ıptico: Parag.

Wyatt and Friesen 2021. Four reference quality genome assemblies of *Pyrenophora teres* f. *maculata*: A resource for studying the barley spot form net blotch interaction. Mol. Plant-Microbe Interact. 34:135-139.

Yoshida, K., Schuenemann, V. J., Cano, L. M., Pais, M., Mishra, B., Sharma, R., Lanz, C., Martin, F. N., Kamoun, S., Krause, J., Thines, M., Weigel, D., and Burbano, H. A. 2013. The rise and fall of the *Phytophthora infestans* lineage that triggered the Irish potato famine. eLife. 2:e00731.

APPENDIX A. CHARACTERISTICS OF GENES IN THE *PTTBEE1* REGION

Gene designator	Start position	Stop position	Transcript length (nucleotides)	Protein length (amino acids)	Predicted secreted by signalp v5.0	Non-classically secreted by deeploc v1.0 or secretomeP v2.0	Predicted effector by effectorP v2.0	Predicted transmembrane domain by TMHMM v2.0	Predicted GPI anchor by netGPI v1.1	Pfam domain identified by Interproscan	RNA coverage
PTT_40000001	3857	4329	472	87	N	N	N	N	N	N	100%
PTT_40000002	4086	4739	653	176	N	N	N	N	N	N	100%
PTT_40000003	6369	10591	4222	933	N	N	N	N	N	Y	100%
PTT_40000004	11721	12155	434	144	N	N	N	N	N	N	100%
PTT_40000005	13739	15940	2201	716	N	N	N	N	N	N	100%
PTT_40000006	106147	106387	240	72	N	N	N	N	N	N	100%
PTT_40000007	112405	112561	156	35	N	N	N	N	N	N	100%
PTT_40000008	129742	131067	1325	407	N	N	N	N	N	Y	100%
PTT_40000009	143642	146716	3074	565	N	N	N	N	N	Y	100%
PTT_40000010	147974	148884	910	197	N	N	N	N	N	N	100%
PTT_40000011	148589	149005	416	122	Y	N	N	N	N	N	100%
PTT_40000012	150667	151299	632	210	N	N	N	N	N	Y	100%
PTT_40000013	151805	153542	1737	545	N	N	N	N	N	Y	100%
PTT_40000014	155070	156095	1025	324	N	N	N	N	N	Y	100%
PTT_40000015	157879	158790	911	303	N	N	N	N	N	N	100%
PTT_40000016	159033	160620	1587	459	N	N	N	N	N	Y	100%
PTT_50000016	147603	147860	257	85	N	N	N	N	N	Y	100%
PTT_40000017	161836	165867	4031	1103	N	N	N	Y	N	Y	100%
PTT_40000018	165766	166329	563	106	N	N	N	N	N	N	100%
PTT_40000019	166352	167440	1088	362	N	N	N	N	N	N	100%
PTT_40000020	167706	168509	803	213	N	N	N	N	N	N	100%
PTT_40000021	202473	212533	10060	3126	N	N	N	N	N	N	100%
PTT_40000022	214719	215246	527	136	N	Y	N	N	N	N	100%
PTT_40000023	215135	217184	2049	403	N	N	N	Y	N	N	100%
PTT_40000024	217603	218367	764	254	N	N	N	N	N	N	100%
PTT_40000025	219602	220479	877	245	N	N	N	N	N	N	100%
PTT_40000026	222466	224259	1793	318	N	N	N	N	N	N	100%
PTT_40000027	224465	225532	1067	254	N	N	N	N	N	Y	100%
PTT_40000028	225621	225824	203	67	N	N	N	N	N	N	100%
PTT_40000029	225869	227599	1730	576	N	N	N	N	N	Y	100%
PTT_40000030	227983	229296	1313	437	N	N	N	N	N	N	100%
PTT_40000031	231485	232118	633	209	N	N	N	N	N	Y	100%
PTT_40000032	233187	234190	1003	326	N	N	N	N	N	N	100%

Gene designator	Start position	Stop position	Transcript length (nucleotides)	Protein length (amino acids)	Predicted secreted by signalp v5.0	Non-classically secreted by deeploc v1.0 or secretomeP v2.0	Predicted effector by effectorP v2.0	Predicted transmembrane domain by TMHMM v2.0	Predicted GPI anchor by netGPI v1.1	Pfam domain identified by Interproscan	RNA coverage
PTT_40000033	234515	235843	1328	442	N	N	N	N	N	N	100%
PTT_40000034	238384	239729	1345	287	Y	N	Y	N	N	Y	100%
PTT_40000035	240093	242144	2051	683	N	N	N	N	N	N	100%
PTT_40000036	244725	245111	386	128	Y	N	N	N	N	N	100%
PTT_40000037	248103	248496	393	81	N	N	N	N	N	N	100%
PTT_40000038	257364	258878	1514	486	N	N	N	N	N	Y	100%
PTT_40000039	260131	261008	877	241	N	N	N	N	N	Y	100%
PTT_40000040	262276	263389	1113	223	N	N	N	N	N	N	100%
PTT_40000041	263573	265602	2029	540	N	N	N	N	N	Y	100%
PTT_40000042	267379	268272	893	189	N	Y	N	N	N	Y	100%
PTT_40000043	269096	270562	1466	488	Y	N	N	N	N	Y	100%
PTT_40000044	270799	271929	1130	358	N	N	N	N	N	N	100%
PTT_40000045	274355	275755	1400	424	N	N	N	N	N	Y	100%
PTT_40000046	276091	279816	3725	1241	N	N	N	N	N	N	100%
PTT_40000047	281207	285972	4765	1580	N	N	N	N	N	Y	100%
PTT_40000048	287323	287589	266	79	N	N	N	N	N	N	100%
PTT_40000049	287875	289657	1782	520	N	N	N	N	N	Y	100%
PTT_40000050	290199	291907	1708	553	N	N	N	N	N	Y	100%
PTT_40000051	292250	293792	1542	495	N	N	N	N	N	Y	100%
PTT_40000052	295933	296509	576	170	Y	N	Y	N	N	N	100%

APPENDIX B. PRIMERS USED FOR MARKER DEVELOPMENT

Primer Name	Primer Sequence
nm1Forward	GACTAGACTAGGGTCTCCCTAGTCTTATCTAATAGCG
nm1Reverse	CGTTCCGATAAGCTTACTACAATAATTAAGTTCGCATCTAGAG
150kbForward	GCTTCTACTAAACAATCAACC
150kbReverse	ACCAAGTAACCTTGTGAGAA

APPENDIX C. AVERAGE REACTION TYPES OF *P. TERES* F. *MACULATA* ISOLATES C-A17, DEN2.6, FGOB10PTM-1, AND P-A14 OBSERVED ACROSS A SET OF TETRAPLOID WHEAT LINES

Line	T. turgidum subsp.	Country	C-A17 avg.	std. dev.	Den2.6 avg.	std. dev.	FGOB10 avg.	std. dev.	P-A14 avg.	std. dev.
2912	durum	China	1.67	0.24	1.50	0.00	1.83	0.24	1.83	0.24
12:61-8T-5T-2aT-2B-2T	durum	Australia	1.67	0.24	1.67	0.24	1.50	0.00	1.50	0.00
2012 M65	durum	Australia	1.25	0.25	1.25	0.25	1.00	0.00	1.00	0.00
2013 M65	durum	Australia	1.00	0.00	1.17	0.24	1.17	0.24	1.00	0.00
2016 M65	durum	Australia	1.33	0.24	1.33	0.24	1.33	0.24	1.17	0.24
Aconhci 89	durum	CIMMYT	1.00	0.00	1.00	0.00	1.17	0.24	1.17	0.24
Agamia	durum	CIMMYT	1.00	0.00	1.17	0.24	1.00	0.00	1.17	0.24
Ajaia 9	durum	CIMMYT	1.83	0.24	1.50	0.00	1.67	0.24	1.67	0.24
Alkabo	durum	ND, USA	2.00	0.00	1.75	0.25	1.83	0.24	1.83	0.24
Allemand	durum	Tunisia	1.25	0.25	1.25	0.25	1.17	0.24	1.17	0.24
Altar 84	durum	CIMMYT	1.17	0.24	1.33	0.24	1.00	0.00	1.00	0.00
Anedj	durum	France	1.33	0.24	1.25	0.25	1.17	0.24	1.00	0.00
ARAOS	durum	CIMMYT	1.67	0.24	1.83	0.24	1.67	0.24	1.67	0.24
Ben	durum	ND, USA	2.50	0.00	2.33	0.24	2.83	0.24	2.50	0.71
Berbern	durum	Tunisia	1.67	0.47	1.83	0.24	1.67	0.24	2.00	0.41
Bidi 17	durum	France	1.33	0.24	1.50	0.41	1.33	0.24	1.50	0.00
Botno	durum	CIMMYT	1.17	0.24	1.25	0.25	1.17	0.24	1.17	0.24
Candeal	durum	Argentina	1.33	0.24	1.33	0.24	1.00	0.00	1.17	0.24
Cappelli	durum	Italy	3.17	0.24	3.33	1.03	2.50	0.41	2.83	0.85
Castiglione Pubescente	durum	Italy	2.17	0.62	3.17	0.24	2.00	0.82	2.17	0.24
Cerceta	durum	CIMMYT	1.17	0.24	1.50	0.00	1.25	0.25	1.00	0.00
CHEN 7	durum	CIMMYT	1.00	0.00	1.00	0.00	1.00	0.00	1.17	0.24
China 34	durum	China	2.50	0.41	1.00	0.00	1.83	0.24	2.00	0.00
Citr3686	dicoccum		2.83	1.65	2.67	0.62	2.33	1.55	3.17	0.62
Cotrone	durum	Italy	1.33	0.24	1.00	0.00	1.00	0.00	1.17	0.24
Croc 1	durum	CIMMYT	1.25	0.25	1.17	0.24	1.00	0.00	1.33	0.24
D 115	durum	France	1.67	0.24	2.17	0.62	1.83	0.85	1.33	0.24
D 73121	durum	Brazil	1.00	0.00	1.50	0.00	1.00	0.00	1.25	0.25
D211	durum	France	2.50	0.41	2.50	0.41	2.50	0.41	2.17	0.24
D304	durum	France	1.83	0.24	2.00	0.00	1.83	0.24	1.75	0.25
Decoy 1	durum	CIMMYT	1.17	0.24	1.67	0.24	1.00	0.00	1.33	0.24

Line	T. turgidum subsp.	Country	C-A17 avg.	std. dev.	Den2.6 avg.	std. dev.	FGOB10 avg.	std. dev.	P-A14 avg.	std. dev.
DG Max	durum	ND, USA	2.17	0.47	2.00	0.41	2.33	0.24	1.75	0.25
DG Star	durum	ND, USA	1.50	0.00	1.50	0.00	1.50	0.41	1.33	0.24
Dilse	durum	ND, USA	2.25	0.75	2.25	0.25	2.00	0.41	2.17	0.24
Divide	durum	ND, USA	2.00	0.00	2.33	0.47	1.67	0.24	2.33	0.62
Doubbi	durum	Australia	1.17	0.24	1.67	0.24	1.17	0.24	1.67	0.24
Durati	durum	Australia	1.17	0.24	1.33	0.47	1.00	0.00	1.33	0.24
Dverd 2	durum	CIMMYT	2.00	0.00	2.00	0.00	1.67	0.24	2.00	0.00
Erythromelan	durum	Poland	1.17	0.24	1.00	0.00	1.17	0.24	1.17	0.24
Falcin 1	durum	CIMMYT	1.00	0.00	1.00	0.00	1.00	0.00	1.00	0.00
Farro Lungo	durum	Italy	1.17	0.24	1.67	0.24	1.00	0.00	1.17	0.24
FHB4512	durum	China	1.33	0.24	1.33	0.24	1.50	0.00	1.17	0.24
Gan	durum	CIMMYT	1.00	0.00	1.00	0.00	1.00	0.00		
Gerardo 624	durum	Italy	2.00	0.00	2.33	0.47	1.67	0.24	1.83	0.24
Giorgio 331	durum	Italy	1.83	0.24	2.33	0.24	1.50	0.41	1.67	0.24
Grande Dora	durum	ND, USA	1.17	0.24	1.33	0.24	1.33	0.24	1.33	0.24
Green 3	durum	CIMMYT	1.00	0.00	1.00	0.00	1.00	0.00	1.00	0.00
Grenora	durum	ND, USA	2.17	0.24	1.83	0.24	1.83	0.24	2.00	0.00
Hordeiforme I	durum	Poland	1.17	0.24	1.17	0.24	1.17	0.24	1.00	0.00
Hordeiforme II	durum	Poland	1.00	0.00	1.17	0.24	1.00	0.00	1.00	0.00
Huguenot	durum	Australia	1.17	0.24	1.17	0.24	1.00	0.00	1.00	0.00
ICM314	durum	Tunisia	1.17	0.24	1.00	0.00	1.00	0.00	1.00	0.00
Israel A	dicoccoides		1.50	0.00	1.75	0.25	1.67	0.24	1.75	0.25
Iumillo	durum	Italy	1.00	0.00	1.33	0.24	1.17	0.24	1.17	0.24
KAPUDE 1	durum	CIMMYT	1.00	0.00	1.17	0.24	1.00	0.00	1.00	0.00
Laidley	durum	Australia	1.83	0.24	2.33	0.47	1.50	0.00	1.67	0.24
Langdon	durum	ND, USA	1.00	0.00	1.33	0.24	1.00	0.00	1.00	0.00
Lebsock	durum	ND, USA	1.33	0.24	1.67	0.24	1.17	0.24	1.33	0.24
Lenah Khetifa	durum	Tunisia	1.00	0.00	1.00	0.00	1.00	0.00	1.25	0.25
Leucomelan Biskrei	durum	Poland	1.17	0.24	1.50	0.00	1.50	0.00	1.00	0.00
Mahmoudi Ag	durum	Tunisia	1.17	0.24	1.17	0.24	1.17	0.24	1.33	0.24

Line	T. turgidum subsp.	Country	C-A17 avg.	std. dev.	Den2.6 avg.	std. dev.	FGOB10 avg.	std. dev.	P-A14 avg.	std. dev.
Medeah	durum	Tunisia	1.50	0.00	1.00	0.00	1.17	0.24	1.00	0.00
Mountrail	durum	ND, USA	1.33	0.24	1.17	0.24	1.17	0.24	1.67	0.24
Muriciense	durum	Poland	2.00	0.00	1.75	0.25	1.83	0.24	1.83	0.24
N-85	durum	China	1.17	0.24	1.17	0.24	1.00	0.00	1.17	0.24
PI 167622	polinicum		1.33	0.24	1.67	0.62	1.00	0.00	1.17	0.24
PI 254206	turanicum		1.67	0.24	1.75	0.25	1.67	0.24	1.67	0.24
PI 352519			1.33	0.24	1.00	0.00	1.17	0.24	1.17	0.24
PI 481521	dicoccoides		1.00	0.00	1.00	0.00	1.00	0.00	1.17	0.24
PI 61102	carthlicum		1.33	0.24	1.50	0.00	1.00	0.00	1.00	0.00
Pierce	durum	ND, USA	1.83	0.24	1.67	0.24	1.67	0.47	1.83	0.24
Realforte	durum	Tunisia	1.33	0.24	1.50	0.50	1.17	0.24	1.33	0.24
Sbei	durum	Tunisia	1.67	0.24	1.67	0.24	2.25	0.25	2.00	0.00
Scaup	durum	CIMMYT	1.33	0.24	1.00	0.00	1.33	0.24	1.50	0.00
Sceptre	durum	Saskatchewan	2.00	0.41	1.83	0.24	2.00	0.00	2.25	0.25
Scoop 1	durum	CIMMYT	1.00	0.00	1.00	0.00			1.00	0.00
SHAG 22	durum	CIMMYT	1.00	0.00	1.00	0.00	1.00	0.00	1.00	0.00
Sincape 90	durum	Italy	1.50	0.00	2.17	0.24	1.83	0.24	2.00	0.41
Sora	durum	CIMMYT	1.83	0.24	1.67	0.24	1.50	0.00	1.67	0.24
Souri	durum	Tunisia	1.17	0.24	1.50	0.41	1.17	0.24	1.17	0.24
Sterna - DW	durum	CIMMYT	1.00	0.00	1.00	0.00	1.00	0.00	1.00	0.00
TA106			1.67	0.24	1.17	0.24			1.67	0.24
Timor	durum	Brazil	1.17	0.24	1.00	0.00	1.17	0.24	1.00	0.00
Trinakria	durum	CIMMYT	2.67	0.62	2.33	0.62	2.00	0.41	2.00	0.00
Tulatai Maitai	durum	China	1.50	0.00	1.17	0.24	1.00	0.00	1.00	0.00
Vallega Zitelli 611	durum	Italy	1.67	0.24	2.17	0.62	1.67	0.24	2.00	0.00
Vallelunga Glabra	durum	Italy	1.67	0.24	1.33	0.24	1.33	0.24	1.50	0.00
Wales	durum	ND, USA	1.67	0.24	1.67	0.24	2.00	0.00	1.50	0.00
Westhope	durum	ND, USA	1.83	0.24	1.50	0.00	1.83	0.24	1.67	0.24
Yar	durum	CIMMYT	1.67	0.24	1.67	0.24	1.67	0.24	1.50	0.41

APPENDIX D. AVERAGE REACTION TYPES OF *P. TERES* F. *MACULATA* ISOLATES C-A17, DEN2.6, FGOB10PTM-1, AND P-A14 OBSERVED ACROSS THE BP025 POPULATION

Progeny	C-A17 avg.	std. dev.	Den2.6 avg.	std. dev.	FGOB10Ptm-1 avg.	std. dev.	P-A14 avg.	std. dev.
1	1.83	0.29	1.17	0.29	1.33	0.29	1.50	0.50
2	1.00	0.00	1.00	0.00	1.00	0.00	1.00	0.00
3	2.00	0.00	1.83	0.29	1.83	0.29	2.17	0.29
4	1.50	0.50	1.50	0.00	1.50	0.00	1.50	0.50
5	1.00	0.00	1.00	0.00	1.00	0.00	1.00	0.00
6	1.17	0.29	1.50	0.50	1.17	0.29	2.00	0.50
7	1.50	0.00	1.50	0.00	1.67	0.29	1.67	0.29
8	1.00	0.00	1.00	0.00	1.00	0.00	1.00	0.00
9	1.67	0.58	1.50	0.00	1.67	0.58	1.67	0.29
10	1.00	0.00	1.83	0.29	1.33	0.29	1.25	0.35
11	1.00	0.00	1.00	0.00	1.00	0.00	1.00	0.00
12	1.00	0.00	1.00	0.00	1.17	0.29	1.00	0.00
13	1.17	0.29	1.00	0.00	1.00	0.00	1.17	0.29
14	1.00	0.00	1.17	0.29	1.17	0.29	1.67	0.29
15	1.50	0.00	1.50	0.00	1.00	0.00	1.50	0.50
16	1.00	0.00	1.00	0.00	1.00	0.00	1.00	0.00
17	1.17	0.29	1.00	0.00	1.17	0.29	1.00	0.00
18	2.00	0.00	1.83	0.29	1.67	0.29	1.83	0.58
19	1.83	0.29	2.17	0.29	1.83	0.29	1.83	0.29
20	1.67	0.29	1.33	0.29	1.83	0.58	1.83	0.29
21	1.33	0.29	1.67	0.29	1.67	0.58	1.83	0.58
22	1.17	0.29	1.00	0.00	1.00	0.00	1.33	0.58
23	1.50	0.00	2.00	0.50	1.67	0.29	1.33	0.29
24	1.33	0.58	1.67	0.29	1.17	0.29	1.50	0.50
25	1.00	0.00	1.00	0.00	1.33	0.29	1.00	0.00
26	1.00	0.00	1.00	0.00	1.00	0.00	1.00	0.00
27	1.00	0.00	1.00	0.00	1.00	0.00	1.00	0.00
28	1.00	0.00	1.00	0.00	1.33	0.29	1.17	0.29
29	1.00	0.00	1.17	0.29	1.00	0.00	1.17	0.29
30	1.00	0.00	1.00	0.00	1.00	0.00	1.00	0.00
31	2.00	0.00	1.83	0.29	1.83	0.29	2.00	0.00
32	1.00	0.00	1.00	0.00	1.17	0.29	1.00	0.00
33	1.33	0.29	1.33	0.29	1.33	0.58	1.67	0.76
34	1.17	0.29	1.50	0.00	1.17	0.29	1.33	0.29
35	1.17	0.29	1.17	0.29	1.17	0.29	1.17	0.29
36	1.83	0.29	2.33	0.29	1.17	0.29	1.67	0.29
37	1.17	0.29	1.00	0.00	1.00	0.00	1.00	0.00

Progeny	C-A17 avg.	std. dev.	Den2.6 avg.	std. dev.	FGOB10Ptm-1 avg.	std. dev.	P-A14 avg.	std. dev.
38	2.00	0.00	2.00	0.00	1.50	0.50	2.50	0.50
39	1.33	0.29	1.17	0.29	1.33	0.29	2.17	0.76
40	1.00	0.00	1.00	0.00	1.00	0.00	1.00	0.00
41	1.50	0.00	1.33	0.29	1.00	0.00	1.83	0.29
42	1.33	0.29	1.17	0.29	1.17	0.29	1.33	0.29
44	1.00	0.00	1.00	0.00	1.00	0.00	1.00	0.00
45	1.17	0.29	1.17	0.29	1.17	0.29	1.50	0.00
46	1.00	0.00	1.17	0.29	1.00	0.00	1.00	0.00
47	1.83	0.29	1.67	0.29	2.00	0.87	2.00	0.50
48	1.67	0.29	1.50	0.00	1.67	0.29	2.00	0.50
49	1.50	0.00	1.50	0.50	1.50	0.00	1.75	0.35
50	1.33	0.58	1.17	0.29	1.50	0.00	1.33	0.29
51	1.67	0.29	1.00	0.00	1.00	0.00	1.33	0.29
52	2.00	0.50	2.00	0.00	2.17	1.15	2.00	0.50
53	1.00	0.00	1.00	0.00	1.00	0.00	1.33	0.29
54	1.17	0.29	1.33	0.29	1.17	0.29	1.33	0.58
55	2.17	0.76	2.67	0.76	2.00	0.50	2.17	0.29
56	1.00	0.00	1.00	0.00	1.00	0.00	1.00	0.00
57	1.00	0.00	1.33	0.29	1.25	0.35	1.67	0.29
58	1.67	0.29	1.67	0.29	1.67	0.29	2.17	0.29
59	1.17	0.29	1.00	0.00	1.17	0.29	1.00	0.00
60	1.83	0.29	2.00	0.00	1.83	0.29	1.83	0.29
63	1.00	0.00	1.00	0.00	1.17	0.29	1.17	0.29
64	1.75	0.35	1.83	0.29	1.33	0.29	2.00	0.50
65	1.67	0.58	1.50	0.00	1.83	0.29	2.17	0.76
66	2.17	0.76	2.83	0.29	2.67	0.29	2.67	0.29
67	1.00	0.00	1.17	0.29	1.00	0.00	1.00	0.00
68	1.00	0.00	1.00	0.00	1.00	0.00	1.00	0.00
69	2.17	0.76	2.83	0.29	2.83	0.29	2.67	0.76
70	1.33	0.29	1.00	0.00	1.17	0.29	1.00	0.00
71	1.33	0.29	1.50	0.00	1.50	0.00	1.67	0.29
72	1.17	0.29	1.33	0.29	1.33	0.58	1.50	0.50
73	1.00	0.00	1.00	0.00	1.00	0.00	1.17	0.29
74	1.17	0.29	1.33	0.29	1.00	0.00	1.17	0.29
75	1.17	0.29	1.00	0.00	1.00	0.00	1.00	0.00
76	1.00	0.00	1.00	0.00	1.00	0.00	1.67	0.58
77	1.00	0.00	1.00	0.00	1.17	0.29	1.00	0.00
78	1.50	0.00	1.50	0.00	1.33	0.58	1.83	0.58
79	2.17	0.29	2.00	0.50	1.83	1.04	2.67	0.58
80	1.00	0.00	1.17	0.29	1.00	0.00	1.00	0.00
81	1.00	0.00	1.00	0.00	1.00	0.00	1.17	0.29
82	1.50	0.00	1.83	0.29	1.67	0.29	1.83	0.29
83	1.00	0.00	1.17	0.29	1.00	0.00	1.17	0.29

Progeny	C-A17 avg.	std. dev.	Den2.6 avg.	std. dev.	FGOB10Ptm-1 avg.	std. dev.	P-A14 avg.	std. dev.
84	1.50	0.50	1.33	0.29	1.50	0.00	2.00	0.00
85	1.17	0.29	1.00	0.00	1.00	0.00	1.00	0.00
86	1.17	0.29	1.00	0.00	1.00	0.00	1.00	0.00
87	1.83	0.29	2.00	0.00	1.83	0.29	2.00	0.00
88	1.00	0.00	1.00	0.00	1.00	0.00	1.17	0.29
89	1.50	0.00	1.50	0.00	1.67	0.29	1.83	0.29
90	1.17	0.29	1.17	0.29	1.33	0.29	1.33	0.29
91	1.00	0.00	1.00	0.00	1.00	0.00	1.00	0.00
92	1.00	0.00	1.00	0.00	1.00	0.00	1.00	0.00
93	2.33	0.58	1.83	0.29	2.00	1.00	2.00	0.87
94	1.17	0.29	1.33	0.29	1.67	0.58	1.50	0.00
95	1.33	0.58	1.50	0.50	1.17	0.29	1.83	0.76
96	1.17	0.29	1.25	0.35	1.50	0.00	1.50	0.50
97	1.50	0.50	1.67	0.29	1.67	0.58	1.50	0.00
98	1.00	0.00	1.00	0.00	1.00	0.00	1.00	0.00
99	1.00	0.00	1.00	0.00	1.00	0.00	1.17	0.29
100	1.17	0.29	1.00	0.00	1.00	0.00	1.00	0.00
101	1.17	0.29	1.67	0.29	1.17	0.29	1.50	0.50
102	1.50	0.00	1.67	0.29	1.67	0.29	1.67	0.29
103	1.67	0.29	1.67	0.29	1.67	0.29	1.83	0.29
104	1.67	0.29	1.50	0.50	1.67	0.29	2.17	0.76
105	1.00	0.00	1.00	0.00	1.00	0.00	1.17	0.29
106	1.00	0.00	1.17	0.29	1.17	0.29	1.33	0.29
107	1.00	0.00	1.00	0.00	1.17	0.29	1.33	0.29
108	1.33	0.29	1.67	0.29	1.50	0.00	1.50	0.50
109	1.83	0.29	1.83	0.29	2.17	0.29	1.83	0.29
110	1.00	0.00	1.50	0.50	1.17	0.29	1.50	0.00
111	1.00	0.00	1.00	0.00	1.00	0.00	1.00	0.00
112	1.50	0.00	1.50	0.00	1.50	0.00	1.33	0.29
113	1.17	0.29	1.33	0.29	1.17	0.29	1.67	0.29
114	1.17	0.29	1.00	0.00	1.33	0.58	1.33	0.58
115	1.67	0.29	2.00	0.50	1.67	0.29	2.33	0.29
116	1.00	0.00	1.17	0.29	1.17	0.29	1.00	0.00
117	1.00	0.00	1.17	0.29	1.00	0.00	1.50	0.00
118	1.67	0.29	1.50	0.00	1.00	0.00	1.83	0.29
119	1.67	0.29	1.50	0.00	1.83	0.29	2.00	0.00
120	1.00	0.00	1.17	0.29	1.00	0.00	1.17	0.29

APPENDIX E. DISEASE REACTION TYPE DATA FOR ALL THREE REPLICATES OF THE GDP SUBSET INOCULATED WITH FGOB10PTM-1

DWRC#	R1	R2	R3	DWRC#	R1	R2	R3	DWRC#	R1	R2	R3
3	1.0	1.5	1.0	674	1.0	1.0	1.0	1211	1.5	1.0	1.5
5	2.0	1.0	1.0	675	1.0	1.0	1.0	1212	1.5	2.0	2.0
7	1.5	1.0	1.5	676	1.0	1.0	1.0	1213	1.5	1.5	3.0
8	2.5	1.5	2.0	679	1.5	1.5	1.0	1218	2.0	2.5	3.5
9	1.5	1.5	2.0	680	2.0	1.5	2.0	1223	1.5	2.0	2.0
11	2.0	1.5	1.0	681	1.5	1.5	1.5	1224	1.0	1.0	1.0
20	2.0	1.5	2.0	682	2.0	1.5	1.5	1225	2.0	1.5	1.0
25	2.0	1.5	1.0	684	1.5	1.5	1.0	1227	2.0	2.0	3.0
26	1.0	1.0	1.0	685	2.0	2.0	2.0	1228		1.5	2.0
27	1.0	1.0	1.0	686	2.0	2.0	2.0	1229	1.0	1.0	1.0
29	1.0	1.0	1.0	687	1.0	1.0	1.0	1230	1.0	1.0	1.0
31	2.5	2.0	2.5	693	2.0	2.0	1.5	1234	1.5	1.5	1.5
32	1.0	1.0	1.0	694	1.5	1.5	1.5	1238	1.0	1.0	1.5
36	1.0	1.0	1.0	695		1.0	1.0	1239	1.0	1.5	1.0
39	1.0	1.0	1.0	696	2.5	2.0	2.0	1241	1.0	1.0	1.0
53	1.5	1.0	1.0	697	1.0	1.0	1.0	1242	2.5	2.0	2.0
54	1.0	1.0	1.0	698	1.5	1.5	1.5	1243	1.5	1.5	3.0
82	1.0	1.0	1.0	702	1.5	1.0	1.0	1244	1.0	1.5	1.0
91	1.0	1.0	1.0	703	2.5	1.5	2.0	1245	1.0	1.0	1.0
110	1.5	1.5	1.5	707	1.0	1.0	1.0	1246	1.0	1.0	1.0
112	2.0	1.5	1.5	709	1.5	1.0	1.5	1247	1.0	1.0	1.0
117	1.5	1.5	1.5	710	1.5	1.5	1.0	1248	1.5	1.0	1.5
118	1.0	1.5	2.0	711	1.5	1.5	1.0	1250	1.0	1.0	1.0
119	2.5	2.0	3.0	712		1.5	1.5	1251	1.0	1.0	1.5
120	1.5	2.0	1.5	713	1.5	1.5	1.0	1258	1.5	1.5	1.0
121	1.0	1.5	1.0	715	1.5	1.0	1.0	1259	1.0	1.5	1.0
123	1.5	1.5	1.0	717	1.5	1.0	1.0	1260	1.5	1.0	1.5
126	3.0	1.5	2.0	718	1.0	1.0	1.0	1261	1.0	1.5	1.0
127	1.0	1.0	1.5	719	2.0	1.5	2.0	1262	1.0	1.0	1.0
128	1.5	1.5	2.0	721	1.5	1.0	2.0	1263	1.0	1.0	1.0
129	1.5	1.5	2.0	722	3.0	1.5	3.5	1265	1.0	1.0	1.5
132	4.0	2.0	2.5	723	2.0	1.0	2.0	1266	1.0	1.0	1.0
139	1.0	1.5	1.0	726	2.5	2.0	2.0	1267	1.0	1.0	1.0
145	1.0	1.0	1.0	728	1.0	1.0	1.0	1268	1.0	1.5	2.5
146	1.0	1.0	1.0	729	3.0	3.0	2.0	1270	1.5	1.5	1.0
152	1.5	1.5	2.0	730	2.0	2.0	1.5	1271	1.0	1.0	1.0
156	1.0	1.0	1.0	731	2.0	2.5	2.0	1277	1.5	1.5	2.0
167	1.5	1.0	1.5	732	1.5	2.0	2.0	1281	1.0	1.0	1.5
169	1.5	1.5	1.0	733	3.0	2.0	2.0	1282	1.0	1.0	1.0
178	1.0	1.0	1.0	734	1.5	1.5	1.0	1283	1.5	1.0	1.0
182	2.0	1.5	2.0	735	1.0	1.0	1.0	1284	1.5	1.5	1.0
188	2.0	1.5	1.5	736	1.0	1.0	1.0	1285	1.0	1.0	1.0
198	1.0	1.0	1.0	737	1.5	1.5	1.0	1287	1.0	1.0	1.5
199	1.5	1.5	2.0	759	1.5	1.0	1.0	1288	1.5	1.5	1.0

DWRC#	R1	R2	R3	DWRC#	R1	R2	R3	DWRC#	R1	R2	R3
212	1.0	1.0	1.0	776	2.5	1.5	2.0	1294	1.0	1.0	3.0
213	2.0	1.0	1.5	779	1.0	1.0	1.0	1298	1.0	1.0	1.0
215	1.0	1.0	1.0	794	2.5	1.5	3.0	1303	2.5	2.0	1.5
216	1.0	1.0	1.0	800	2.0	2.0	2.5	1304	1.5	1.5	1.0
218	1.5	2.0	1.5	805	1.5	1.5	2.0	1305	2.0	2.0	1.5
219	1.5	1.0	1.5	807	1.5	1.5	3.0	1306	5.0	4.5	5.0
230	3.0	2.0	1.0	809	1.5	1.5	1.5	1308		2.5	1.5
236	1.5	2.0	1.5	810	1.0	1.0	1.0	1310	2.5	1.5	2.0
237	1.5	1.0	1.0	813	1.5	1.0	2.0	1312	1.0	1.0	1.0
238	1.0	1.0	1.0	814	2.0	1.0	1.5	1313	2.0	1.5	2.0
240	2.0	1.5	2.5	824	2.0	1.0	2.5	1314	1.5	2.0	1.0
241	1.5	2.0	2.0	839	1.0	1.0	1.0	1315	2.5	3.0	3.5
242	1.0	1.0	1.0	842	1.5	1.0	1.0	1316	1.5	1.5	2.5
243	1.0	1.0	2.0	846	2.5	2.5	3.0	1318	2.0	1.5	1.5
244	3.0	1.5	3.0	848	1.5	2.0	2.0	1321	1.5	1.0	2.0
246	1.0	1.0	1.5	849	1.5	1.5	1.0	1325	1.0	1.0	1.0
249	1.5	1.5	1.5	854	2.0	1.0	1.0	1327	3.0	2.5	2.5
251	1.0	1.0	1.0	858	1.5	1.5	1.0	1328	1.5	1.5	1.5
252	1.0	1.0	1.5	863	3.0	1.5	1.5	1329	1.5	1.0	1.0
255	1.0	1.0	1.0	867	3.5	1.5		1331	1.0	1.0	1.5
256	1.0	1.0	1.0	868	1.5	1.5	2.0	1332	1.0	1.0	1.0
257	1.5	1.5	2.0	870	1.0	1.0	1.0	1333	1.5	1.0	1.0
258	1.5	2.0	1.5	872	1.0	1.0	1.5	1334	1.5	2.0	2.0
259	1.0	1.0	1.0	875	1.0	1.0	1.0	1336	1.0	1.5	1.5
265	1.5	2.0	1.0	878	1.0	1.0	1.0	1337	2.0	2.0	1.5
266	1.5	1.0	1.5	880	1.0	1.5	1.0	1338	1.0	1.5	1.5
269	1.5	1.5	1.0	881	1.5	1.5	1.5	1339	1.5	1.5	2.0
272	1.0	1.0	1.0	885	1.0	1.0	1.0	1343	1.5	1.5	1.5
273	1.0	1.0	3.0	890	2.5	2.0	2.0	1346	1.5	1.0	1.0
276	1.5	1.0	1.0	894	1.0	1.0	1.0	1354	1.5	2.0	1.0
277	2.0	1.5	2.0	896	1.5	1.5	2.0	1355	1.5	2.0	1.5
279	1.5	1.5	2.5	897	1.5	2.0	2.5	1357	1.5	1.5	1.0
280	1.5	1.5	2.0	899	2.5	1.0	1.0	1358	1.0	1.5	2.0
281	1.5	1.0	2.5	901	1.0	1.0	1.0	1360		1.0	1.0
282	2.0	2.0	2.5	914	1.5	1.5	1.5	1361	1.0	2.0	1.0
284	2.5	2.0	2.0	919	1.0	1.0	1.0	1366	1.0	1.5	1.0
285	2.0	1.5	2.5	929	1.5	1.0	1.5	1368	1.5	1.5	1.5
286	1.0	1.5	1.5	931	2.0	2.0	3.5	1370	2.5	2.0	2.5
287	2.0	1.0	2.5	932	1.5	1.5	1.5	1374	2.0	2.0	2.0
288	1.5	1.5	2.0	934	1.0	1.0	1.0	1375	1.0	1.0	1.0
289	1.5	1.5	2.5	936	1.0	1.0	1.0	1376	1.5	1.5	2.0
290	1.0	1.0	1.5	944	2.5	1.5	1.5	1378	1.0	1.0	1.0
291	1.0	1.0	1.0	951	1.5	2.0	2.0	1379	1.0	1.0	1.0
295	2.0	2.0	2.0	962	1.0	1.0	1.5	1380	2.0	2.0	3.0
296	1.0		1.0	968	1.0	1.0	1.0	1383	3.0	2.0	3.0
299	1.5	1.5	1.5	970	1.5	1.5	2.0	1386	2.0	2.5	2.0
301	2.0	1.5		976	1.0	1.0	1.0	1393	1.0	1.0	1.0
303	1.5	1.5	2.0	979	1.5	1.0	1.0	1398	1.5	1.0	1.0

DWRC#	R1	R2	R3	DWRC#	R1	R2	R3	DWRC#	R1	R2	R3
304	2.0	2.0	2.0	981	2.0	2.0	2.0	1399	1.5	1.0	1.0
305	1.0	1.0	1.0	988	2.5	2.0	2.0	1401	1.5	1.0	1.0
306	2.0	2.0	2.0	989	1.5	1.5	1.5	1402	2.0	1.5	1.5
308	1.0	1.5	2.5	991	1.5	1.0	1.5	1403	1.0	1.0	1.0
309	1.0	1.5	1.0	1007		1.5	2.0	1404	1.0	1.0	1.0
311	1.5	1.5	1.5	1008	1.5	1.5	1.0	1405	1.0	1.0	1.5
313		1.0	1.0	1012	1.0	1.5	1.0	1407	1.0	2.0	1.0
317	2.5		3.0	1014	1.0	1.0	1.5	1408	2.0	1.5	2.0
324	1.0	1.0	1.0	1022	1.0	1.0	1.0	1409	1.0	1.0	1.5
325	1.0	1.0	1.0	1024	1.0	1.0	1.5	1414	1.0	1.0	1.5
327	1.0	1.0	1.0	1032	2.0	2.0	2.0	1416	1.0	1.5	1.5
340	1.5	2.0	2.5	1035	1.5	1.5	2.0	1417	1.0	1.5	1.0
343	1.0	1.0	1.0	1036	1.0	2.0	1.5	1425	1.5	1.0	1.5
344	1.0	1.0	1.0	1038	2.0	3.0	1.5	1426	1.0	1.0	1.0
345	1.0	1.0	1.0	1040	1.5	1.0	1.0	1434	2.0	1.5	2.0
346	1.0	1.0	1.0	1041	1.0	1.0	1.0	1435	1.0	1.0	1.0
347	1.5	2.0	1.5	1045	1.0	1.0	1.0	1437	1.0	1.0	1.0
352	1.5	2.0	1.5	1049	1.5	1.5	1.5	1439	1.5	1.0	1.5
355	1.5	1.0	2.0	1053	1.0	2.0	3.0	1441	1.0	1.0	1.5
356	1.0	1.0	1.0	1054	1.0	1.0	1.0	1442	1.0	1.0	1.0
366	1.0	1.0	1.0	1057	1.0	1.0	1.0	1443	2.0	1.5	2.0
367	1.5	2.0	1.0	1059	2.0	1.5	1.5	1500	1.5	1.5	1.5
374	1.0	1.0	1.5	1061	1.5	1.5	1.0	1502	1.0	1.0	1.0
379	1.5	2.5	1.5	1063	1.0	1.5	1.0	1507	1.0	1.0	1.5
381	2.0	1.5	1.5	1067	2.0	1.5	2.0	1509	1.0	1.0	1.0
394	2.0	1.5	1.5	1070	1.0	1.0	1.0	1510	1.0	2.0	1.5
400	1.0	1.0	1.0	1072	1.0	1.0	1.5	1512	1.0	1.0	1.5
405	1.0	1.0	1.0	1077	1.0	1.5	2.0	1513		2.0	1.5
417	2.0	2.0	1.5	1081	1.0	1.0	1.0	1516	1.0	1.0	1.5
427	1.0	1.0	1.0	1083	2.0	2.0	1.5	1518	1.5	2.0	1.5
433	1.0	1.0	2.5	1091	1.0	1.0	1.0	1520	2.5	2.5	2.0
435	1.5	1.0	2.5	1097	1.0	2.0	2.5	1904	1.0	1.0	1.0
446	1.5	1.5	2.0	1100	1.5	1.5	1.0	1905	1.0	1.0	2.0
451	1.0	1.0	1.0	1103	1.0	1.0	1.0	1906	1.0	1.5	1.0
474	1.5	1.0	1.5	1104	1.5	1.5	1.5	1908	1.5	1.5	2.0
499	1.5	1.5	2.5	1105	1.0		1.0	1911	1.5	1.0	1.0
507	1.5	1.0	1.0	1108		1.0	1.5	1913	1.0	1.0	1.0
508	2.0	2.0	1.5	1111	1.5	1.0	2.0	1914	2.0	1.5	1.5
509	2.0	2.0	1.0	1116	1.0	1.0	1.0	1915	1.5	2.0	1.5
511	1.5	1.0	1.0	1117	1.5	1.0	1.0	1916	2.5	2.0	2.5
512	2.0	1.5	1.5	1120	1.0	1.0	1.0	1917	1.0	1.0	1.0
517	1.0	1.0	1.0	1121	1.0	1.0	1.0	2025	4.0	4.0	4.0
526	1.0	1.0	1.5	1122	1.0	1.5	1.0	2026	1.0	1.5	1.5
535	1.0	1.0	1.5	1126	1.0	1.5	1.0	2029	1.0	1.0	1.0
551	2.0	2.0	1.5	1127	1.0	1.0	1.0	2032	1.0	1.5	1.5
558	2.0	2.0	1.5	1129	1.0	1.0	1.0	2043	1.5	1.5	1.5
564	1.5	1.0	1.5	1130	1.0	2.0	1.0	2046	1.5	1.5	2.0
567	2.0	1.5	1.0	1141	1.5	1.0	2.0	2063	1.0	1.0	1.5

DWRC#	R1	R2	R3	DWRC#	R1	R2	R3	DWRC#	R1	R2	R3
568	1.5	1.0	2.0	1147	1.5	3.0	2.0	2065	1.0	1.0	1.5
578	1.5	1.0	1.0	1149	2.5	2.0	3.0	2067	1.0	1.0	1.0
579	2.0	1.5	2.0	1150	1.5	1.5	1.5	2072	1.5	1.0	1.0
580	2.5	1.5	2.0	1153	1.0	1.0	1.5	2078	1.0	1.0	1.5
590	1.5	1.0	1.0	1157	2.0	2.5	1.0	2081	1.0	1.5	1.0
592	1.0	1.0	1.5	1158	1.5	1.5	2.0	2082	1.5	1.0	1.5
594	1.5	1.0	1.0	1161	1.5	1.5	2.0	2087	1.0	1.0	1.0
596	2.0	1.5	1.0	1163	1.0	1.0	1.5	2095	1.5	1.5	2.0
598	1.5	2.0	1.5	1164	1.5	1.0	1.0	2099	1.0	1.0	1.5
601	1.0	1.0	1.0	1165	1.5	2.0	2.0	2100	1.0	1.0	1.0
604	1.0	1.0	1.5	1166	1.5	2.0	2.0	2102	1.5	1.0	1.5
609	1.0	1.0	1.5	1168	1.0	1.0	1.0	2104	1.5	1.0	1.0
610	1.0	1.0	1.0	1175	1.0	1.0	1.5	2110	1.0	1.5	1.5
611	1.5	1.5	1.5	1179	2.0	2.0	1.5	2114	1.5	1.0	1.5
622	2.0	1.5	1.5	1182	1.5	1.0	1.0	2120	3.0	2.0	2.5
623	1.5	1.0	1.5	1183	1.0	1.0	1.0	2121	1.5	1.0	1.5
625	1.0	1.0	1.0	1185	3.0	2.0	3.0	2122	2.0	1.0	1.0
629	2.0	1.5	1.5	1186	3.5	2.5	3.0	2129	1.5	1.5	1.5
631	1.0	1.0	1.0	1193	2.0	1.5	2.0	2131	1.0	1.0	1.0
632	1.5	1.0	1.0	1195	1.5	1.5	1.0	2132	1.0	1.0	1.0
637	2.0	1.0	1.0	1196	2.0	2.5	1.0	2164	3.0	2.0	2.5
638	2.0	1.5	1.5	1197	1.0	1.0	1.0	2171	1.0	1.0	1.0
639	1.0	1.0	1.0	1198	1.5	1.0	1.0	2184	1.5	1.5	1.0
641	1.0	1.0	1.5	1199	2.0	1.5	2.0	2194	1.5	1.0	1.0
643	2.0	1.5	1.5	1201	1.5	2.0	2.0	2206	1.5	1.0	1.5
652	1.5	1.5	1.5	1202	2.0	2.0	1.5	2213	1.0	1.0	1.0
654	2.5	2.0	1.5	1203	1.0	1.0	1.0	2232	1.0	1.0	1.0
656	2.0	1.5	1.5	1208		1.5	1.5	2243	1.5	1.0	1.0
673	1.0	1.5	1.5	1209	2.5	3.5	4.0	2248	2.0	1.5	2.0
								2261	1.5	1.5	1.5
								2285	2.0	1.0	1.0
								2288	1.0	1.0	1.0

APPENDIX F. QTL DATA REPRESENTING ASSOCIATIONS IN THE DURUM WHEAT GENOME WITH SUSCEPTIBILITY/RESISTANCE TO *P. TERES* F. *MACULATA* ISOLATES

Isolate	Chromosome	Position (cM)	LOD	R^2	LOD threshold
C-A17	2A	24	5.4	19%	3.35
Den2.6	2A	22	3.4	13%	3.26
FGOB10Ptm-1	2A	22	7.4	25%	3.27
P-A14	2A	26	4.0	15%	3.37

Data created using composite interval mapping with forward cofactor selection. LOD thresholds based on 1,000 permutations with an $\alpha = 0.05$ level of significance.